International Journal of Extreme Manufacturing

TOPICAL REVIEW • OPEN ACCESS

Biofabrication strategies with single-cell resolution: a review

To cite this article: Dezhi Zhou *et al* 2023 *Int. J. Extrem. Manuf.* **5** 042005

OPEN ACCESS
IOP Publishing | IMMT
International Journal of Extreme Manufacturing
Int. J. Extrem. Manuf. 5 (2023) 042005 (29pp)
https://doi.org/10.1088/2631-7990/ace863

Topical Review

Biofabrication strategies with single-cell resolution: a review

Dezhi Zhou[1,2,3], Bohan Dou[1,2,3], Florian Kroh[1,2,3], Chuqian Wang[1,2,3] and Liliang Ouyang[1,2,3,*]

[1] Department of Mechanical Engineering, Tsinghua University, Beijing 100084, People's Republic of China
[2] Biomanufacturing and Rapid Forming Technology Key Laboratory of Beijing, Tsinghua University, Beijing 100084, People's Republic of China
[3] 'Biomanufacturing and Engineering Living Systems' Innovation International Talents Base (111 Base), Tsinghua University, Beijing 100084, People's Republic of China

E-mail: ouy@tsinghua.edu.cn

Received 14 February 2023, revised 28 March 2023
Accepted for publication 18 July 2023
Published 9 August 2023

Abstract

The introduction of living cells to manufacturing process has enabled the engineering of complex biological tissues *in vitro*. The recent advances in biofabrication with extremely high resolution (e.g. at single cell level) have greatly enhanced this capacity and opened new avenues for tissue engineering. In this review, we comprehensively overview the current biofabrication strategies with single-cell resolution and categorize them based on the dimension of the single-cell building blocks, i.e. zero-dimensional single-cell droplets, one-dimensional single-cell filaments and two-dimensional single-cell sheets. We provide an informative introduction to the most recent advances in these approaches (e.g. cell trapping, bioprinting, electrospinning, microfluidics and cell sheets) and further illustrated how they can be used in *in vitro* tissue modelling and regenerative medicine. We highlight the significance of single-cell-level biofabrication and discuss the challenges and opportunities in the field.

Keywords: cellular building block, modular assembly, single-cell resolution, *in vitro* model, regenerative medicine

1. Introduction

The diverse function of natural organisms is highly related to their heterogeneous structure and composition. As an interdisciplinary technology, biofabrication provides reliable strategies for the manipulation and positioning of cells and biomaterials to recapitulate the native counterpart. The traditional bulk biofabrication approaches usually exhibit poor controllability over component distribution. Biofabrication strategies based on modular assembly use cells and materials as building blocks to construct desired patterns or structures, demonstrating their potential in various biomedical applications, such as *in vitro* tissue modeling and regenerative medicine [1, 2].

With a closer look at the native tissues at the cell scale, one can find that many tissues exhibit cellular structures with fine features down to single cell level (figure 1). For

* Author to whom any correspondence should be addressed.

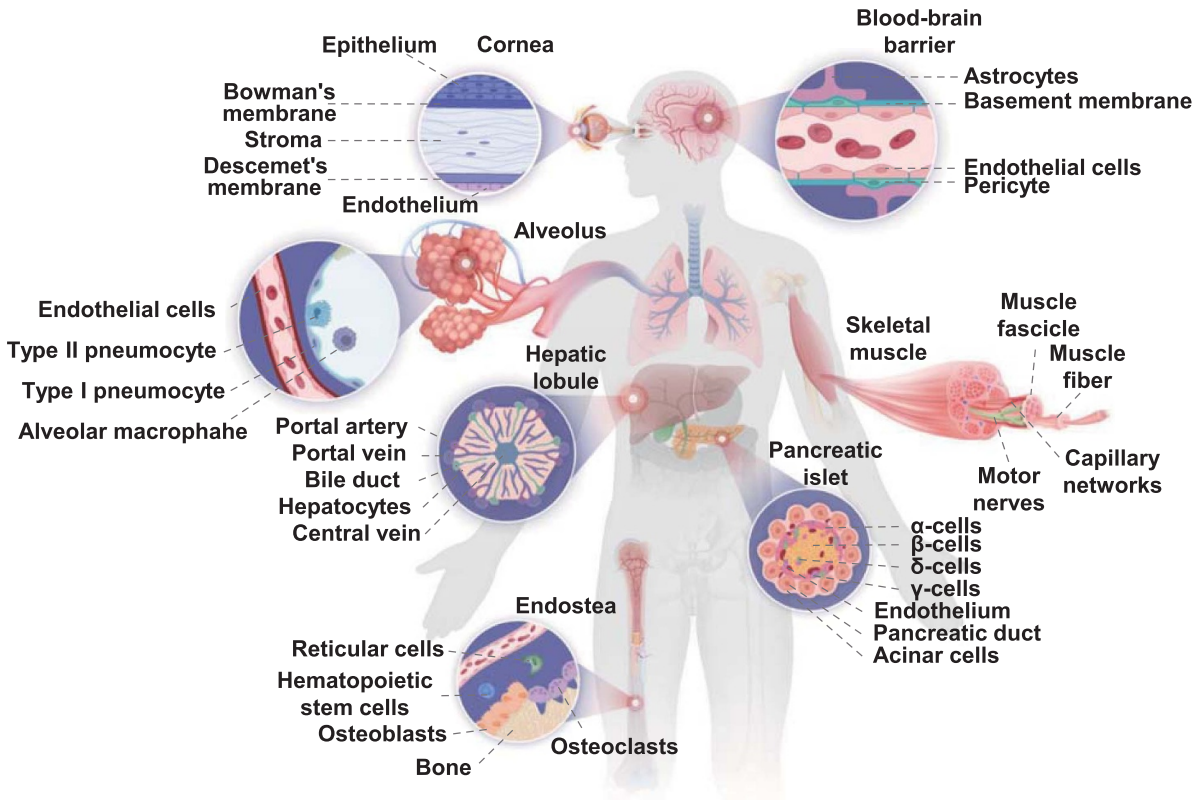

Figure 1. Illustration of representative tissues/organs with heterogeneous construction at single-cell scale.

example, pancreatic islets are composited of at least five types of cells, which form spacial junctions locally within a dimension of several cells. The tight and orderly structure allows cell–cell interaction and maintains the blood glucose homeostasis [3]. Skeletal muscle is a typical anisotropic tissue containing bundled muscle fascicles encased by the epimysium. The vascularized and innervated muscle fascicles exhibit the normal function by order transition between relaxation and contraction [4]. Alveolus is another example, which presents multi-layer walls surrounded by a network of capillaries for gas exchange. The unique topological structure and the multi-layer air-blood interface with a few micrometers of thickness provide a large surface (100–140 m^2) for effective gas exchange [5]. These heterogeneous structures with cell-scale features are vital in native tissues, which, however, are difficult to engineer *in vitro* when using cell populations as the building materials. The spontaneous and time-consuming cell self-assembly within the engineered cellular scaffold further adds to the difficulty in recapitulating heterogeneity precisely. On the other hand, due to the heterogeneity within the same cell population, high-throughput platforms with single-cell resolution are necessary to facilitate the exploration of single-cell analysis. Therefore, the development of biofabrication strategies with single-cell resolution will greatly contribute to both *in vivo* and *in vitro* tissue engineering applications.

In the past decade, biofabrication technology has been seen with numerous progress, including those achieving single-cell resolution [6–8]. For example, accurate controllability over the separation and deposition of single cells can be achieved by cell trapping or single-cell printing for single-cell analysis and cellular behavior study. The assembly of single-cell filaments is also possible for the precise fabrication of anisotropic tissues such as muscle and nerve, while the assembly of monolayer cell sheets is available for multilayer tissue fabrication. These building blocks can be regarded as basic units that can be assembled orderly to construct higher-order architectures. Thus, according to the dimension of the smallest structural building blocks, we categorize the biofabrication strategies with single-cell resolution into three types, i.e. zero-dimensional (0D) (single-cell droplets), one-dimensional (1D) (single-cell filaments), and two-dimensional (2D) (single-cell sheets) (figure 2).

Past review articles have summarized the advances in single-cell printing or patterning [9–11], and others have highlighted the general modular assembly [12, 13]. There is no available review summarizing all kinds of biofabrication techniques (beyond bioprinting) that achieve single-cell resolution (beyond single-cell manipulation), nevertheless covering the applications in biomedicine. We believe it is timely and necessary to comprehensively overview the available biofabrication strategies with single-cell resolution and their applications. Herein, we focus on the modular assembly of cellular building blocks with single-cell features and classify these biofabrication strategies according to the dimension of the building blocks. It starts with an informative introduction to the advances of different biofabrication techniques.

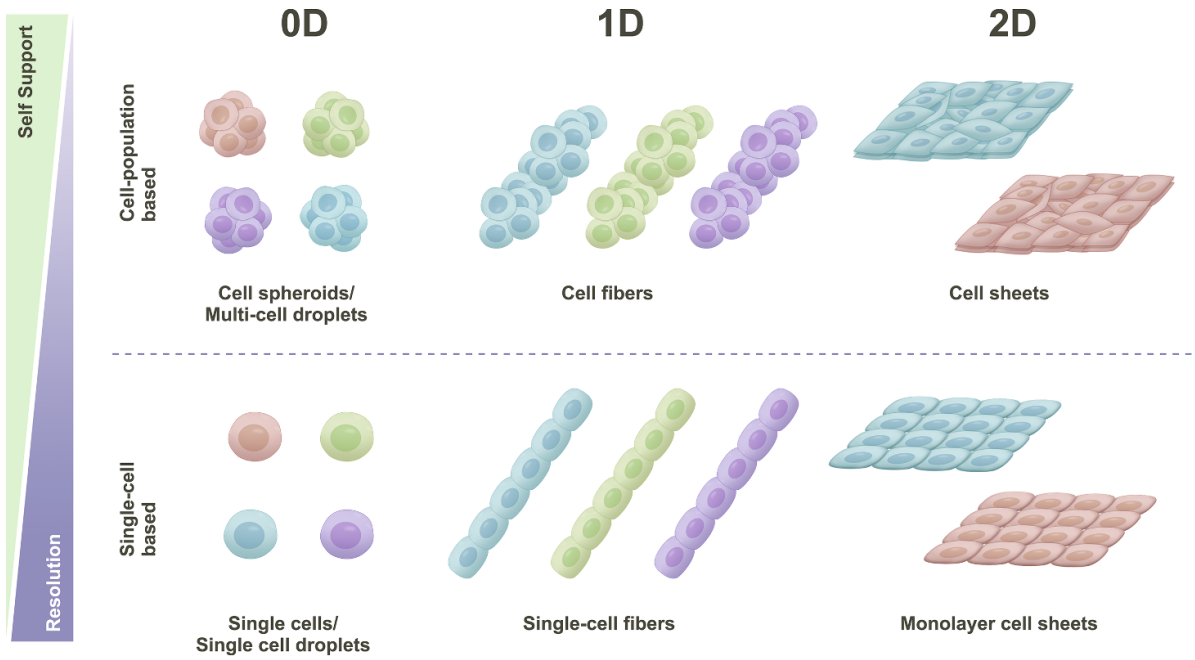

Figure 2. Illustration of cell-population- and single-cell-based building blocks at different dimensions.

In this part, we introduce their mechanisms, most recent advances, advantages, and disadvantages. Then we introduce how these biofabrication strategies with single-cell resolution can be used in *in vitro* tissue modelling and regenerative medicine, illustrated by providing the most recent examples. We intend to inspire the researchers in the field by overviewing these advances and providing our perspectives throughout the manuscript.

2. Biofabrication of building blocks with single-cell resolution

2.1. 0D cellular building blocks with single-cell resolution

The separation of a single cell from the cell population is the initial step to obtain a 0D building block. Utilization of a single-cell size barrier for trapping is a straightforward strategy that also enables programmed pattering of these single cells. The barrier trap can be divided into two types, i.e. interface barrier trapping (figure 3(a)) and free single-cell trapping (figure 3(b)). Interface barrier trapping relies on stencil preprocessing or surface modification to form patterns for selective cell immobilization, while the free single-cell trapping applies a certain force to assemble cells selectively. Another promising strategy is single-cell printing (figure 3(c)) which generates single-cell building blocks and deposits them in the pre-design location. The emergence of microfluidic techniques (figure 3(d)) further improves the capacity of generating single-cell building blocks, enhancing the efficiency of single-cell printing.

2.1.1. Interface barrier trapping

2.1.1.1. Stencil. The stencil technique separates and positions the single cells via the constraint of a topological structure, which is usually a trap of a single-cell size scale (figure 3(a)-i). The advances in microfabrication technologies (e.g. photolithography, soft lithography, and laser ablation) have enabled the creation of a stencil with micro-scale features [14] and facilitated its use in single-cell related applications.

A typical stencil trapping device with microwell arrays can be manufactured by sticking a through-hole stencil to a substrate. When cell suspension is poured to fill the generated wells, only a single cell can pass through and occupy each well due to the size limitation. For example, Wu *et al* attached a Si-stencil with a through-hole array (the smallest diameter is 8 μm) closely to the surface of the culture dish to establish the isolated residence for single cells [15]. The connection among the isolated rooms can be easily achieved by modifying the stencil structure while maintaining the single-cell traps. In another study, Li *et al* fabricated a polydimethylsiloxane (PDMS) stencil with a neat through-hole structure in which each hole was surrounded by micropillars (3 μm in height). Due to the supporting micropillars, the single neurons within the individual wells can connect with each other to form a neuron network [16]. A more straightforward approach is to template a stencil using a complementary mold with inverse structures. Soft lithography is a widely used technique to fabricate molds with microstructures, while PDMS, a biocompatible elastomer with high transparency,

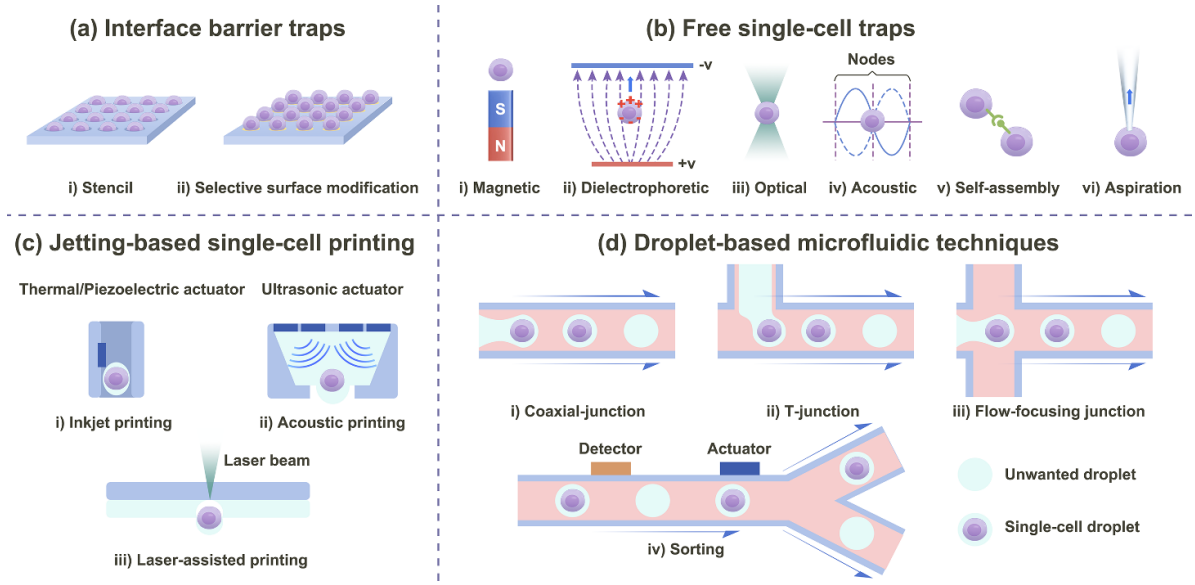

Figure 3. Schematic of enabling techniques for 0D single-cell building block manipulation. (a) Stencil preprocessing or surface modification establishes the interface barriers for selective cell trapping. (b) Various types of forces are used to assemble cells selectively. (c) Jetting-based printing techniques are used to deposit single-cell droplets. (d) Microfluidic techniques are used to produce and sort single-cell droplets.

is usually cast to generate the stencil [17]. In this manner, Huang *et al* fabricated a cone-shaped microwell array chip and successfully trapped single cells in individual microwells [18]. Microspheres have also been used as molds to template spherical traps, which eliminates the time-consuming procedure of soft lithography [19, 20]. For example, Liu *et al* immobilized polystyrene microspheres onto the plasma-treated glass substrate via heating and used it as a mold [20].

Although stencil provides a delicate trap for capturing single cells, the spontaneous occupancy of cells remains a challenge. Additional steps, such as centrifugation [18] and flow [21], can be introduced to facilitate the occupancy and maximize the occupancy ratio.

2.1.1.2. Selective surface modification. Selective surface modification via physicochemical techniques can form custom patterns that guide cell adhesion (figure 3(a)-ii), where the manipulation of cells is indirectly achieved via patterning the bonding materials such as adhesion molecules [22] and DNA [23].

Microcontact and noncontact approaches are both used to generate the pattern on the substrate. Microcontact printing usually applies the micro stamp to transfer the precursor solution onto the substrate, where the resultant pattern is a replicate of the stamp. It is worth mentioning that the cell-laden precursor can be directly stamped to form a single-cell array, but the cell concentration is vital. Xu *et al* found that the lower cell concentration benefited the formation of single-cell spots but reduced the occupancy ratio of cells in the array [24]. Higher cell concentration seems beneficial for better occupancy but might induce multi-cell aggregation in one spot. To avoid multi-cell capturing, Bhujbal *et al* suggested that the suitable size of a single spot should be half of the cell diameter. To maintain a clear separation of individual cells on an array, they further suggested the smallest distance between adjacent spots twice the cell size [25]. In the typical stamping process, the substrate usually holds higher surface energy than the stamp in order to attract the stamping ink molecules. In a reverse process, stamps with high surface energy peel off a pattern of the ink molecules on the substrate in a subtractive manufacturing manner. For example, Wu *et al* coated a hydrophilic polydopamine layer onto the hydrophobic glass and then applied an oxygen plasma–activated PDMS stamp to obtain a negative polydopamine pattern [26]. The resultant molecular patterns highly replicated the geometry of the stamp with complex microstructures. The microcontact stamping approach can well replicate the design, but each unique pattern requires the fabrication of a corresponding stamp, and the contact processing may introduce potential contamination that might affect the further cell culture or analysis.

Interface barrier trapping strategy usually induces less damage to cells because the pre-processing of barriers does not involve living cells. However, the delicate process of barriers with single-cell resolution is required to achieve successful trapping of a single cell.

2.1.2. Free single-cell trapping

2.1.2.1. Magnetic trapping. Magnetic objects can be manipulated by the magnetic force of a tunable magnetic field in a contactless way (figure 3(b)-i). Since most living cells do not possess magnetic properties, the paramagnetization of

cells is necessary for magnetic control. Typical magnetic biomaterials used to guide cells include magnetic nanoparticles [27], magnetoferritin [28], liposomes [29, 30], coupling paramagnetic beads [31], magnetic hydrogels [32] and paramagnetic medium [33, 34]. With the proper magnetic configuration, the magnetic field can isolate single cells from cell populations. For example, Durmus *et al* successfully distinguished different types of cells based on their density via the magnetic system [34]. To trap the cells to form patterns, Ino *et al* established a pin holder device composited of magnetic pillars to attract the magnetically labelled cells. The resolution is limited due to the multiple cell aggregation induced by the large area of the pillar (100 μm in diameter) [35]. It is practical to reduce the magnetic interaction area with approximate size to the diameter of a single cell for single-cell trapping. For example, Pivetal *et al* successfully patterned the magnetically labeled *Escherichia coli* bacteria ($\sim$2 μm) with a magnetic array composited of 5 μm wide metal stripes [36]. Although many studies have proven the temporal biocompatibility of different magnetic materials, it still risks long-term cytotoxicity, especially when using a high dose [29, 33]. Further, the magnetic field ($\sim$1 T) with a high gradient (up to 1 GT/m) has been demonstrated to significantly change the membrane potential of cells and thus to affect cell function [37]. Therefore, careful optimization of magnetic materials and parameters is important for cell manipulation.

2.1.2.2. Dielectrophoretic trapping. Dielectrophoretic trap refers to the use of dielectrophoresis to separate and manipulate particles including living cells. When a neutral but polarizable particle is placed under an inhomogeneous electric field, the particle movement occurs due to the interaction between the induced dipole within the particle and the spatial gradient of the electric field [38]. This dielectrophoretic trapping force is highly dependent on the applied electric field, electrical properties of the medium, and the size and shape of the particle, while has little to do with the charge of the particle [39]. When the interaction area between the cell and electric field is confined to the scale of cell size, single-cell manipulation is possible (figure 3(b)-ii). Hunt and Westervelt successfully adopted a glass tip surrounded by dielectrophoretic force as a tweezer in single-cell manipulation and the trapped cell divided normally [38]. For single-cell pattering, the patterned electrodes can guide the trapped cells to form a corresponding pattern, but the geometry of the electrodes and properties of the cells (e.g. size) and medium (e.g. conductivity and viscosity) should be properly considered [40, 41]. For example, strong electric fields may bring irreversible damage to cells, including those caused by current-induced Joule heating of the medium and changes in transmembrane potentials [41, 42]. Using an electric field with a frequency of $\sim$MHz, reducing the duration and intensity of exposure fields can help reduce cell damage [40, 41].

In the dielectrophoretic trapping approach, the medium used should possess good cytocompatibility. The physicochemical properties of the medium should also be considered. For example, less-viscous mediums contribute to the fast movement of particles, enabling efficient cell patterning [40]. Moreover, to achieve multiple single-cell manipulations, independent control of each electric field by individual electrodes is required. To achieve a precise and individual switch of the electrodes, Yang *et al* introduced an optically tunable phototransistor array that offers the manipulation of single cells out of the dielectrophoresis trap via the illumination of phototransistors [43].

2.1.2.3. Optical trapping. Optical tweezers emerged as a non-contact tool for trapping a microparticle and transferring it spatially (figure 3(b)-iii). It requires a highly focused laser beam that exerts the scattering force and the gradient force determined by the laser beam (intensity and wavelength) and the target particle (shape and size). The scattering force pushed the object towards the beam propagation, and the gradient force pulls it into the center of the focal plane, which maintains the stable trap [44, 45]. Due to these properties, non-spherical and too-large particles would cause an elusive situation of scattering and gradient forces. A recent report proved that the optical trap can manipulate an otolith of 55 μm in diameter within a larval zebrafish [46].

Since a free single cell exhibits a spherical shape with a micro-scale (mostly $\sim$10 μm), it is a suitable object for optical tweezer trapping. For example, Ashkin *et al*., for the first time, applied the optical tweezer to confine and freely move the single cell at velocities of 100 μm s^{-1} in water without obvious cell damage [47]. Later, Liu *et al* demonstrated that the laser would cause a heating effect on the target cells [48]. Laser with a wavelength from 700 to 760 nm was reported to cause unfavorable influences on clone growth in the Chinese hamster ovary [49] and the stress response in *Caenorhabditis elegans* [50]. Additionally, the effects on cell growth and proliferation are compounded by increasing exposure time and laser power [49, 51]. Therefore, proper optimization of laser configurations (e.g. wavelength, power, and exposure time) is vital to minimize the damage to cells. Converging other techniques with optical tweezers is an option to leverage the challenges. For example, Wu *et al* developed an optoelectronic tweezer technique to achieve the manipulation of single cells, in which the optical images are applied to trigger dielectrophoresis electrodes for further manipulating single particles via an electric field. This approach combined the advantages of dielectrophoresis and optical tweezers, requiring less optical intensity than the optical tweezers alone [52, 53]. In another study, Probst *et al* combined microfluidics with optical tweezers to save the time of manipulation. They designed a microfluidic channel to deliver the cell via flow to a temporary position, then the optical tweezers just need to trap and move it to the target chamber [54]. In summary, the optical trap shows advantage in precise controllability of single cells, but might induce potential cell damage.

2.1.2.4. Acoustic trapping. The acoustic trap is a technique that relies on sound waves to precisely manipulate particles ranging from nanometers to millimeters in a

non-contact manner (figure 3(b)-iv). Compared to the magnetic and optical trapping techniques, the acoustic trap is free of particle labelling and laser-induced damage. Further, the sound waves can propagate along with solid, liquid, and gas, which makes the acoustic trap a versatile tool. The potential damage of acoustic waves to cells or tissue is caused by the resultant heating or cavitation effects [55]. With proper parameters, the acoustic damage of cells is negligible. For example, Sundvik *et al* evaluated the effect of acoustic waves on zebrafish embryos, and the results showed no significant difference in viability and development between the non-acoustic and acoustic (treated for 2000 s) groups [56]. Another study also proved that the viability of red blood cells can be maintained during 30 min of acoustic tweezer treatment [57].

In acoustic tweezers, single-cell manipulation is mainly achieved by the surface acoustic wave [58]. Ding *et al* located the interdigital transducers on the surface of a piezoelectric substrate to generate standing surface acoustic waves for patterning single red blood cells and manipulated single *C. elegans* [59]. Briefly, the movement of the cell relies on the orthogonal surface acoustic waves which form pressure nodes in their overlapped nodes to trap the cell and then carry it to the next node (figure 3(b)-iv). Therefore, the resolution of displacement is mostly determined by the distance between two pressure nodes, which can be tuned by the acoustic wave frequency. Furthermore, a wavelength on the approximate order of the captured cell diameter is required to promise a single cell in the pressure node [60]. Apart from the plane pattering of single cells, the 3D manipulation of a single cell is possible for the surface acoustic waves. For example, Guo *et al* established a 3D trapping system by propagating orthogonal surface acoustic waves through a fluid-filled chamber where an additional acoustic field caused acoustic streaming to generate vertical displacement [61]. The displacement of these 3D trapping nodes can be precisely controlled by altering the phase angles of each interdigital transducer pair (horizontal direction) and the input acoustic power (vertical direction), respectively. Recently, a novel strategy was adopted to achieve spatial manipulation of a single cell [62]. This system relies on the spiraling electrodes metallized on the surface of a piezoelectric substrate to generate a focused acoustical vortex triggered by a function generator. Subsequently, a single cell was selectively trapped within the spherical vortex while the mobile platform drove the chamber to alter the relative position of the captured cell. This study suggests that using a movable platform may be an alternative to alleviate the challenge of manipulating the acoustic waves spatially.

2.1.2.5. Single-cell self-assembly. Cells exchange biophysical and biochemical signals to communicate in a well-organized 3D microenvironment, which has crucial implications in various cellular functions such as cell cycle regulation and differentiation fate. The contact-dependent interaction between cells is especially important for tissue formation. Inspired by these characteristics, *in vitro* single-cell self-assembly can be achieved via molecular recognition and biological interactions [12]. To achieve precise and selective manipulation of cells, special recognition between the target cells is vital (figure 3(b)-v). Gartner and Bertozzi functionalized the target cells with complementary single-stranded DNA (ssDNA) to establish a DNA-mediated reversible system where the single cells can combine or dissociate both in cell-friendly conditions [63]. With this regard, the cells functionalized with different sequences of ssDNA can self-assemble in a layer-by-layer manner to form spatial cellular structure via the iteration of this process [23]. Recently, Ge *et al* established DNA origami nanostructures to replace the ssDNA strands for cell self-assembly [64]. They managed to use the DNA origami nanostructures to assemble T cells and tumor cells to form asymmetric and directional arrangements by establishing biomimetic membrane channels for cell–cell communications. Apart from DNA-based materials, various molecules have also been applied to modify the cell for special recognition such as biotin–streptavidin [65], bio-orthogonal chemical groups [66], and antibodies [67]. The cells' self-assembly process is highly dependent on the cell types and the adhesion molecules. Recently, Stevens *et al* generated synthetic cell adhesion molecules by combining orthogonal extracellular interactions with intracellular domains from native adhesion molecules [22]. With this synthetic cell adhesion molecules tool, they further demonstrated the potential of extracellular interaction domains in controlling the cell connection. Gene engineering can also help the cells obtain special recognition. For example, blue light-triggered proteins, CRY2 and CIBN, can be expressed on the surfaces of cells and these proteins can form reversible bonding to control cell self-assembly with visible light illuminating [68]. The modification process of cells to obtain self-assembly properties can be gentle and biocompatible, but cell functionality should be further evaluated after modification. Since the assembly relies on the self-activating identification of cells, external stimuli that cause cell damage can be minimized.

2.1.2.6. Aspiration-based trapping. Aspiration-based trap relies on the aspiration forces caused by the negative pressure within a microcapillary to capture the particles (figure 3(b)-vi). The aspiration technique has been used to catch and isolate a single cell from the cell population [69]. To successfully trap a single cell, the nozzle size of the microcapillary should be smaller than the diameter of the cell. Combining an aspiration-based trap with a mobile platform enables the transfer and localization of trapped cells. For example, Hacohen *et al* successfully trapped a single cell with a tiny tip and assembled the single cell one by one to form a 2D pattern [70]. To construct a 3D structure, immobilization of the cells spatially is fundamental. Moreover, a cell-friendly environment with adequate humidity and nutrient should be maintained to support cell survival during assembling. Recently, a suspension supporting bath used in extrusion-based 3D printing has shown superiorities in the structure support and nutrient supplement owing to the self-healing and water-rich properties of the batch [71]. With this strategy, Ellison *et al* managed to deposit different single cells to form a spatial and heterogeneous structure

within a microgel suspension bath [72]. Although such studies have declared the cells maintain viable after trapping [71, 72], more investigations are needed to clarify the minimum aspiration force to transfer but not damage the single cells. This issue may relate to the surface tension coefficient of the medium-cell interface, cell radius, and tapered angle of the capillary [73].

2.1.3. Jetting-based single-cell printing. Jetting-based printing is an effective technology to generate and deposit droplets with a volume down to picoliter in a non-contact manner. The droplets can be generated either in a continuous or drop-on-demand way. Due to the superiority of accuracy and printing speed, jetting-based techniques have been applied in cell printing, and researchers have widely demonstrated the maintenance of cell viability [74–77]. Typical jetting-based printing techniques for single-cell printing are illustrated in figure 3(c).

To achieve single-cell printing, one needs to optimize some critical parameters, such as cell concentration, printing configurations, and ink properties. For example, Xu *et al* found that, in inkjet printing, inks with high cell concentration can lower the proportion of empty droplets as well as that of the single cell droplets, leading to more droplets with multiple cells [78]. This is also the truth with other jetting-based printing techniques such as electrostatic inkjet printing [74], laser-induced forward transfer [79, 80], valve-based printing [81], acoustic printing [77] and alternating viscous and inertial force jetting [82, 83]. Unsurprisingly, the containing cell number is also highly dependent on the size of the droplet, which correlates with the printing parameters and ink properties [84, 85]. During the jetting process, a narrower nozzle enables fewer volume of ink flow to form a smaller droplet, which is more likely to carry a single cell. However, narrow nozzles might cause clogging and fatal damage to cells due to high shear force (especially when jetting high-viscosity ink). As for the nozzle-free jetting techniques, the droplet size can be tuned by the corresponding configurations, such as laser power or spot area in laser-induced forward transfer printing [79] and acoustic wave frequency in acoustic printing [77, 86]. For example, Zhang *et al* focused the ultrashort near-infrared laser with a wavelength of 1030 nm into a cell-laden solution where the high photon density within the focus area induced an optical breakdown to generate an expanding cavitation bubble for jetting the cells [87]. With this method, cells within a radius of about 25 μm around the laser focus can be selected for jetting and single-cell printing was achieved by manually locking a target cell under microscopy.

Although micro droplets with a single cell size can be generated, it is still challenging to effectively encapsulate one cell in one droplet due to the Poisson distribution law. Statistical models can be used to predict the distribution based on critical parameters (e.g. cell concentration, droplet size, and cell size) [88]. However, such prediction is usually inaccurate due to the mismatch of actual conditions, such as inhomogeneous distribution of cells in inks caused by cell segmentation. A droplet monitoring system should be more reliable to ensure single-cell encapsulation. For example, Feng *et al* established a detecting and printing system to achieve 100% single oocyte droplet generation based on an impedance detection system [89]. When an oocyte is approaching the jetting zone, it first passes through two electrodes, which sense the entry of the cell and trigger the ejecting action. Only when the oocyte flowed to the jetting zone, the airflow was applied to eject. Using a similar technique, Schoendube *et al* printed HeLa cells and achieved 73% $\pm$ 11% efficiency of single cell ejection [90]. The difference in single-cell efficiency between these two studies is likely due to the size difference of cells (150–180 μm and $\sim$10 μm in diameter for oocyte HeLa, respectively).

In another study, Koltay *et al* applied a computer vision system to dynamically detect the locations of single cells before printing [91], which guides the printer to only jet the single-cell droplet to the target location and dispense the unwanted droplets to the waste area. Due to the random distribution of cells, a large area should be imaged for detection, which led to a heavy calculation and a high waste ratio of ink. To further improve the printing speed and reduce the number of unsuitable droplets, Koltay *et al* introduced an acoustophoresis to position the cells in line [92]. In this manner, smaller detecting regions of interest shorten the calculation time and reduce the waste ratio from 52% $\pm$ 6% to 28% $\pm$ 1%. Nevertheless, the possible stacking or aggregation of cells along the depth of the image would lead to a certain proportion of droplets with multiple cells. Wang *et al* aligned cells in a flowing channel towards the jetting nozzle, where a high-speed camera was set to monitor the flowing. Once a single cell was detected, it would be jetted as a single-cell droplet, and the final proportion of single-cell droplets increased to 90.3% [93]. Such an optical monitor technique is also compatible with other jetting-based printing techniques [94, 95].

A feedback system for recycling the jetted but unqualified droplets can further improve the single-cell proportion. Recently, Zhou *et al* developed an acoustic jetting system that allowed pushing the liquid upwards to absorb the unqualified droplet from the receiver. This is possible by utilizing a strong body force at the resonator-liquid interface induced by a gigahertz acoustic resonator [95]. The liquid overcame the surface tension and was then raised to form a spike, which would either jet a droplet or recycle it from the receiver. Furthermore, this technique allowed for secondary jetting to remove the unwanted droplet on the same location via an optic feedback loop system and finally achieved 100% single-cell droplet patterning. However, this contact method has difficulty in removing the crosslinked droplets, and thus limits its application in 3D structure fabrication which requires droplets gelation and adhesion. Thus, recycling the droplets (e.g. via absorption [95, 96] or backflow to a reservoir [97]) before landing on the substrate seems a more practical strategy for 3D fabrication. Additionally, the incorporation of advanced detecting systems will add to the efficient selection of single-cell droplets from heterogeneous samples based on the cell shape [98, 99] or fluorescence [97, 100, 101]. Furthermore, Riba *et al* demonstrated the use of machine learning in selecting the cells which are likely to clone as the ink for ejection [98].

The relationship between the single cell shape before printing and that at later cloning state was established by analyzing their images, so the cell with higher potential in cloning can be selected and ejected.

Together, jetting-based printing is a promising technique to achieve single-cell resolution biofabrication, and the introduction of a detecting system facilitates the drop-on-demand printing of single cells.

2.1.4. Droplet-based microfluidic technology. The principle of droplet-based microfluidic technology is to apply two co-flowing immiscible fluids to create an interface where one separates into the discrete phase (i.e. droplets) surrounded by the continuous phase (figure 3(d)). With the help of soft lithography, microfluidic devices with fine channels can be fabricated, which makes it possible to generate microdroplets of cell size. Theoretically, cells experience stress from the microfluidic channels during flow. To ease the impact of stress, the channels are usually slightly larger than a single cell, and short channels can be used to reduce the duration of stress. Early studies had proven the feasibility of capturing a single cell within a droplet [102] while cells maintained viability after 2 h [103]. However, according to the Poisson distribution law based on cell random distribution, the highest proportion of single-cell droplets is limited to 37% [104, 105]. Different methods have been exploited to increase this proportion.

Similar to the jetting-based approach, a straightforward approach is to align cells orderly before they enter the junction of the fluids. For example, Kemna *et al* managed to sequence the cell one by one within a continuous curved rectangular microchannel where the cells suffered from the Dean force and the lift force [106]. In this manner, the cells were well-ordered before entering the interface of the oil and water phases, and subsequently, a single cell was captured within a droplet. Due to the different spacing between cells, the single-cell encapsulation ratio limits to no more than 77%. To avoid empty droplet generation, selective crosslinking of cell-laden droplets is a feasible way. For example, Mooney *et al* pre-coated cells with calcium carbonate nanoparticles and mixed them with an alginate solution as the water phase for droplet generation [107]. The droplets containing cells were selectively crosslinked triggered by the release of calcium from the treatment of acetic acid in the oil phase. In contrast, cell-free droplets could be removed easily as they were not crosslinked. In this manner, the proportion of single-cell encapsulation can reach 90%, while the rest usually contained multiple cells [108].

To further sort out the single-cell droplets, a differential detection system can be incorporated into droplet-based microfluidic technology, as used in jetting-based approaches [90]. Depending on the design of the microfluidic channels, droplets with different internal [109] or external structures [110] can be generated. Therefore, single-cell-laden droplets can form core-shell [111] or multi-compartment structures [112] to obtain heterogeneity. Notably, the off-center location of cells within droplets would cause cells to escape during further culture or assembly [108]. The cells can recenter before the gelation of droplets in dynamic environments such as a shaker [108] and fluidic channel [105]. The timing of this delay crosslinking is critical as it might introduce secondary deviation caused by the gravity [113]. Droplet-based microfluidic technology enables the generation of a heterogeneous droplet with a specified cell number [101], which is hardly achieved via typical jetting-based printing techniques. The integration of droplet-based microfluidic and jetting-based printing technologies should add to the capacity of single-cell biofabrication.

2.2. 1D cellular building blocks with single-cell resolution

Fibrous biomaterials have been demonstrated to guide cell alignment and have been utilized in anisotropic tissue engineering [114]. In the context of engineering precise cellular heterogeneity in anisotropic tissues, cellular microfibers with single-cell resolution are particularly important. In this part, we carefully define the 1D living building blocks and introduce different approaches to generating and assembling such blocks with single-cell resolution (figure 4). The 1D block can be assembled by arranging 0D blocks continuously along one direction, so, technically, the techniques of 0D block generation can be used to generate 1D blocks and these techniques would be not repeated here.

2.2.1. Molding. Molding is a straightforward approach to fabricating 1D cellular filaments, the dimension of which is determined by that of the molds (figure 4(a)). Microchannel and microgroove are commonly used for cellular filament generation by filling the precursor into their microstructure. However, the infilling of solution with poor mobility (i.e. high cell density or high-viscosity materials) is challenging, especially when the channels and grooves are narrow [115]. Neal *et al* established a compaction strategy to generate an aligned cellular fiber ($\sim$100 μm) with high cell density [116]. In this process, the fibrinogen precursor was filled into the channel within the gelatin mold (containing crosslinking agents, thrombin) which dissolved when the temperature increased from 4 °C to 37 °C and the cell density increased indirectly due to the decreasing diameter of fibrinogen hydrogel induced by the compaction from gelatin solution. Nevertheless, this strategy still faces challenges in generating cellular filaments with single-cell features. The molding technique enjoys advantages in recapitulating intricate patterns without additional assembly, but the usually difficult extraction of fine microfibers makes it less applicable in directly producing cell-laden 1D building blocks. To alleviate this challenge, cell attachment on the surface of filaments is an alternative. For example, Saeki *et al* managed to generate the gelatin microfibers ($\sim$15 μm) which were crosslinked by glutaraldehyde and washed before co-culture [117]. After mixing the fibroblasts with these pre-fabricated fibers, cells attached to the fiber surface, forming cellular filaments with nearly single-cell resolution.

2.2.2. Extrusion bioprinting. Extrusion bioprinting, which enables the formation of 2D patterns or 3D structures by depositing 1D fibers orderly, is a widely used biofabrication

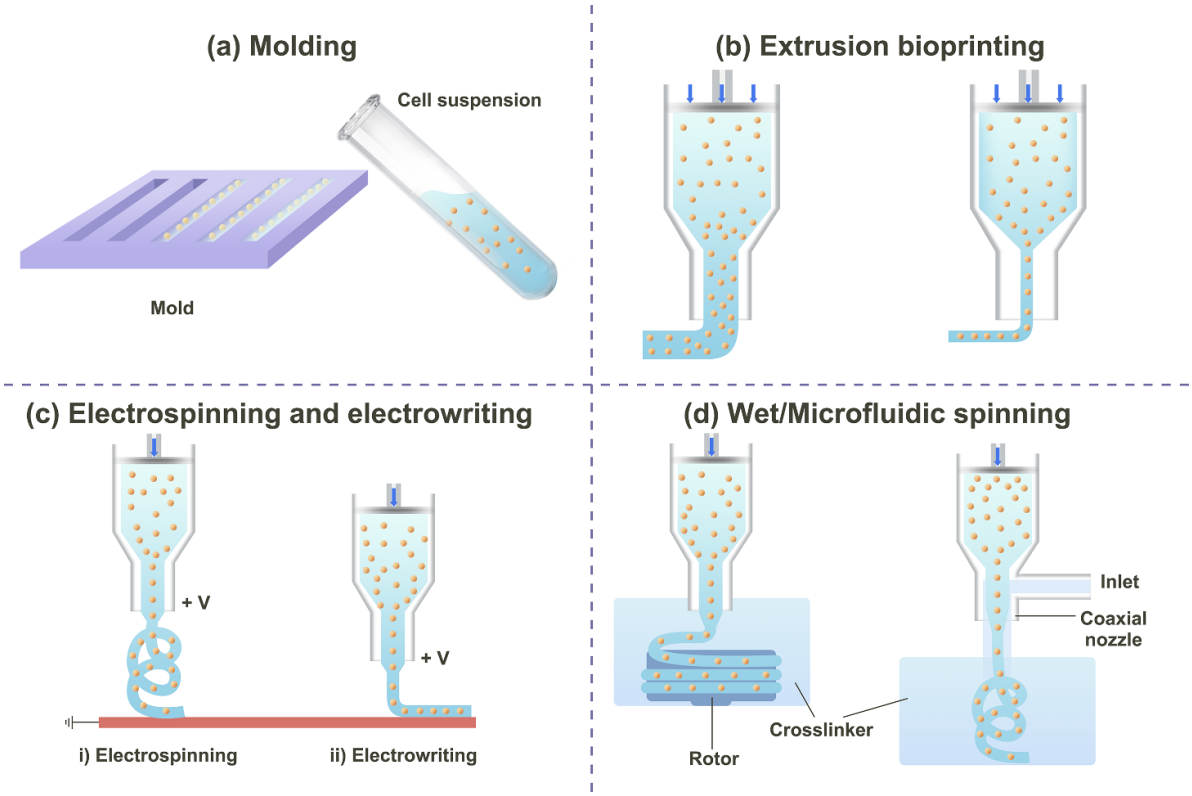

Figure 4. Schematic of enabling techniques for 1D single-cell building blocks manipulation. (a) Molding technique relies on the pre-fabricated mold with single-cell features to confine the seeded cells to form a cellular filament or channel. (b) Extrusion bioprinting uses a tiny nozzle down to cell scale for fine cellular filament generation. (c) Electrospinning and electrowriting techniques apply the electric field to help pull the bioink for single-cell filament generation. (d) Wet/microfluidic spinning introduces the rotor or coaxial flow to help lessen the diameter of the cell-laden filament.

technology owing to its applicability to various ink formulations [118] and easy access [119]. In this approach, continuous filaments are generated and deposited by extruding the bioinks through a tiny nozzle, all in a computer-controlled manner (figure 4(b)). Complex filaments can be engineered by using unique nozzles, such as coaxial filaments with a coaxial nozzle [120] and heterogeneous filaments with pre-set nozzle [121]. Despite these advantages, extrusion bioprinting faces an enduring challenge of generating fine filaments down to cell size. Typically, the bioinks used in extrusion bioprinting need to be viscous enough to maintain the fidelity of filaments [118]. Too narrow nozzles might induce the clog of cell-laden bioinks and cell damage due to a high shear force [122, 123]. *In-situ* photo-crosslinking at the nozzle site was introduced to allow for the bioprinting of low-viscosity bioinks; filaments down to 60 μm in diameter can be printed by using correspondingly small nozzle [124].

More recently, bioprinting in a shear-thinning and self-healing suspension bath has strongly improved the fabrication capacity of extrusion bioprinting [71]. The suspension medium functions as a constraint to encapsulate and support the bioinks, while its self-healing property enables the nozzle to move freely. With this approach, low-viscosity cellularized bioinks can be printed. In addition, Jeon *et al* showed that the suspension medium composed of smaller granules could further benefit a smaller filament generation owing to a decrease of bioink dispersion in fine granules [125]. The use of low-viscosity bioink significantly reduces the shear force to the cell, leading to the possibility of using a smaller nozzle for high-resolution printing. Secondly, adjusting the feeding rate of the bioink and the moving speed of the needle can create a filament smaller than the needle via dragging. For example, Lee *et al* managed to print collagen filaments of 20–200 μm in diameter within the suspension baths by tuning the printing parameters [126].

Despite the advances, it is challenging for low-viscosity bioinks to generate single-cell aligned filaments with a narrow nozzle, which is probably due to cell aggregation and sedimentation. Fathi *et al* demonstrated that cell aggregation and sedimentation dominate the in-nozzle cell movement in culture medium-based bioink (nozzle diameter $<$100 μm), while a cell-laden bioink with certain viscosity (100 mPa·s) exhibited well-dispersed properties and maintain stable printing for tens of minutes [127]. However, such a viscosity might risk potential damage to cells when the cells pass through the narrow tip. Therefore, a versatile system to avoid cell aggregation and sedimentation of low-viscosity bioinks would benefit the printing resolution and cell viability.

2.2.3. Electrospinning and electrowriting. Electrospinning and electrowriting are versatile techniques for generating nano/microscale fibers [128, 129]. They rely on the electrohydrodynamic effects between two distinctly charged electrodes

(i.e. connected to a nozzle and a substrate, respectively) to generate thin fibers from the nozzle (figure 4(c)). The strength of the electric field and the flow rate of ink materials are significant parameters that determine the ink printing to be either pulsating (droplets generation) or continuous (fiber generation) mode [130]. In continuous mode, the ink gets stretched to form a Taylor cone on the nozzle tip as the electric field force overcomes the surface tension, leading to the jetting of fibers smaller than the nozzle. During the deposition of the fibers, the distance between the nozzle and substrate can be modulated to achieve either electrospinning (several centimeters to tens of centimeters) or electrowriting (500 μm to 3 mm), the latter of which allows for considerable control over positioning single fiber [131].

The electric current seems to be a hazard for direct cell printing; the excessive electric current (>50 mA) with an applied voltage of 230 V would cause cell damage due to cell electroporation [132]. Using an insulating substrate (e.g. glass) can effectively lower the electric current to microamperes and even nanoamperes [133, 134]. Previous studies have demonstrated the feasibility of living cell printing with electrohydrodynamic processing techniques. For example, Jayasinghe *et al* successfully printed the Jurkat cell without clogging while maintaining considerable cell proliferation (1.6–2.2 folds) in 24 h [135]. In another study, they further demonstrated the feasibility of electrospinning single-cell encapsulated filament with a coaxial needle where cell suspension is in the core and the PDMS is in the shell [136]. The following studies proved the compatibility of cell inks with high cell concentration (5×10^7 cells ml^{-1}) in electrospinning [137] and the cell activities such as apoptosis and protein expression were demonstrated to present no significant differences between electrospinning and non-treated groups, both *in vivo* and *in vitro* experiments [132, 138]. To better assemble these cellularized microfilaments, a rotating collector [139] or parallel electrodes can be applied to align the filaments anisotropically in electrospinning [140].

To further improve the controllability of these filaments for complex construction, electrowriting is applied as a cell printing method with single-cell resolution. For example, He *et al* precisely fabricated a ten-layer structure composited of continuous cell-laden filament (<100 μm), which can encapsulate a single cell in cross section via adjusting nozzle moving speed and the ink feeding rate [133]. The low surface tension benefits the formation of the Taylor cone and reduces the diameter of jetting filament [141], while the high viscosity reduces the possible generation of beads in the fibers [140]. The inclusion of polyethylene oxide (PEO) in the inks can help hydrogel solutions such as silk, gelatin and alginate to better form continuous filaments [142–144]. For example, Qiu *et al* managed to print complex hexagonal pore structures formed by cell-laden filaments of 30 μm in diameter by incorporating PEO with alginate-based ink [141]. Notably, the introduction of a crosslinking agent (e.g. Ga^{2+} for alginate crosslinking) or the inadequacy of gelation may cause the swelling of filaments. Photocrosslinking is an alternative mechanism to achieve rapid gelation, which also plays an important role in supporting the next layer deposition in 3D. For example, Castilho *et al* functionalized the gelatin and silk to obtain the photocrosslinkable inks which can be printed into spatial structures composited of single-cell filaments (from 5 to 40 μm in diameter) [144]. It is worth mentioning that the hydrogel substrate used in this study can protect the cell-laden filaments from dehydration and provide nutrients for cell survival during the printing process.

Generally, both electrospinning and electrowriting can generate 2D patterns based on 1D microfibrous building blocks, whereas electrowriting is more common in fabricating intricate patterns or 3D architectures. Deformation and collapse are the main challenges for these microfibrous structures in clinical applications due to their weak mechanical properties. Hybrid scaffolds provide a win–win method, in which nano/micro filaments provide the cell-favor microenvironment for growth and function, while the robust structures with larger features provide mechanical support. At present, the incorporation of fused deposition modeling techniques with cell electrospinning/electrowriting is proven to be a potential [145–147]. Furthermore, the combination of electrospinning/electrowriting may further enhance the capacity of hierarchical scaffold fabrication [148]. With the use of robot systems integrating measuring, planning, and execution functions, printing can better adapt to curved surface manufacturing [149]. Overall, electrospinning and electrowriting techniques offer a charming tool for single-cell filament generation but face challenges in controlling surface tension (too high surface tension would cause unstable jetting with bead formation) and developing electric-sensitive biocompatible ink formulations.

2.2.4. Wet spinning and microfluidic spinning. In wet spinning, continuous filaments are formed within the interface of the dynamic liquid flows with immiscible properties (figure 4(d)). Due to the mild and possibly aqueous processing conditions, wet spinning benefits the generation of cell-laden filaments. Typically, cell-containing solutions are extruded into an aqueous bath and then get solidified before the cells diffuse to the surrounding bath. Therefore, slow gelation of precursor solutions might compromise the fidelity of filaments and causes cell leakage due to a non-negligible diffusion. Owing to the rapid and gentle ion crosslinking mechanism, alginate is widely used in wet spinning and can be mixed with other biomaterials such as collagen [150], chitosan [151] and gelatin [152].

A typical wet spinning system uses a rotating collector to drag and collect the continuous microfiber in crosslinking. Such a process may cause breakage of the microfiber on the nozzle tip at high flow velocity due to the mismatch of precursor flow and bath flow directions. Coaxial flow is a widely used approach to form stable laminar flow, which allows for the generation of either solid or hollow filaments. By perfusing crosslinking agent solution through the shell channel, thin filaments (down to 100 μm) can be generated in the core by optimizing the core-shell flow ratios [151]. The filament diameter decreased with the decrease of the core flow rate or the increase of the shell flow rate. The thinning of hydrogel

fibers is also contributed by the dragging effect of the outer stream [153]. When crosslinker solutions are perfused through the core channel and the hydrogel precursor solution flows through the shell channel, a hollow filament can also be generated. In a constant shell flow rate, decreasing the inner flow rate can form a smaller hollow filament [154].

Microfluidic technique has been incorporated in wet spinning for better control over the flow. For example, Yamada *et al* used a microfluidic system to produce a sandwich-like filament with a single-cell scale core (8–12 μm) where aligned single cells were encapsulated [155]. This was possible with the parallel laminar flow between two alginate layers within a rectangular microchannel. To maintain the parallel laminar, they used dextran as the thickener in the shell layer and set a buffer layer between the core and shell layers to moderate the gelling speed of alginate to avoid clogging. The introduction of microfluidic techniques allows the spinning of filaments with various structures such as straight, helical, knot-containing [156], and multicomponent filaments [157]. Recently, Takahashi *et al* used a microfluidic device with multichannels to generate non-cellular thin filaments (8–28 μm in diameter) from a square-shaped channel (100 μm $\times$ 150 μm) where the alginate solution flow was squeezed by the $CaCl_2$ solution from the surrounding channels [158]. Although the squeezing effect is induced by the liquid solution, it remains unknown regarding its effect on cells to evaluate its feasibility in cell-laden material. Nevertheless, wet/microfluidic spinning is still a useful technique to generate 1D building blocks with single-cell resolution. For the fabrication of large and complex structures, these filaments can be assembled to form higher-order 2D patterns or 3D cellular structures via weaving, reeling, knitting, and stacking techniques.

2.3. 2D cellular building blocks with single-cell resolution

2.3.1. Digital light processing. Digital light processing is a photocuring-based 3D printing technique, using dynamic mask photolithography for fabrication. In this approach, the light source is reflected as pattern light by the digital micromirror device or a projector to crosslink a layer of photocurable ink materials with a customized pattern [159] (figure 5(a)). Theoretically, the single-cell resolution in the z-direction of the printed object can be obtained by slicing the digital model into thin layers. However, Kim *et al* found that the hole features lower than 200 μm in the z dimension may lose after printing [160], which suggests the possible relationship between the light penetration depth and the resolution in the Z direction. Apart from layer thickness, bioink composition and printing parameters (e.g. light exposure time, light intensity) can be optimized to improve the printing resolution. For example, Zhu *et al* managed to print a cell-free vascular network with different diameters (5–50 μm) at different Z heights [161]. However, as for the printing of cell-laden materials, the introduction of cells can cause scattering to lower the resolution; the smallest feature of cell-laden structure is 50 μm [161]. Similar to other light-based fabrication techniques, parameters such as intensity and exposure of laser can be adjusted to minimize cell damage. In all, digital light processing is a promising printing technique, but more efforts are needed to generate cellular architecture with single-cell features in the z-direction.

2.3.2. Cell sheet techniques. Cell sheet technique provides a scaffold-free strategy for biofabrication. After seeding onto a culture dish, adherent cells can grow and form a tightly connected monolayer on the culture surface. With various separation strategies, the cellular monolayer can be detached as a cell sheet for secondary manufacturing of multi-layer structures. Therefore, the monolayer cell sheet can be regarded as a 2D building block with single-cell resolution. In this section, we will introduce the generation techniques and assembly strategies of cell sheets (figure 5(b)).

2.3.2.1. Thermoresponsive surface for cell sheet generation. Cell detachment could be achieved by culturing cells on a surface coated with thermoresponsive materials and changing the temperature (figure 5(b)-i). Poly(N-isopropylacrylamide) (PIPAAm) is the most common thermoresponsive material in cell sheet generation due to its temperature-induced transition of hydrophilicity and hydrophobicity. In 1990, Okano *et al* first demonstrated the successful formation and detachment of a cell sheet on a PIPAAm-grafted surface without a typical enzymatic treatment [162, 163]. With a lower critical solution temperature of 32 °C, PIPAAm exhibits hydrophobicity at 37 °C and forms a stable surface for cell sheet formation. When decreasing the temperature below 32 °C, PIPAAm becomes hydrated and soluble with an extended chain conformation, and the cell sheet thus detaches from the substrate [164]. To enhance the cell growth on this synthetic polymer, cell adhesive peptides and growth factors can be introduced to the PIPAAm layer [165]. Dzhoyashvili *et al* found that the thickness of a cell sheet is dependent on the PIPAAm-grafted layer [166]. By tuning the PIPAAm layer thickness, they were able to obtain a monolayer endothelial cell sheet. However, the previous studies also demonstrated that a thinner PIPAAm layer would benefit cell adhesion but led to inadequacy detachment [167]. To alter the thickness of PIPAAm layer after cell seeding, one could apply an elastic substrate and mechanical stress [168]. This method relies on the stretch of the elastic substrate to thin the layer, which promotes cell adhesion to form cell sheets rapidly. Then the shrinking of the elastic substrate can accelerate the detachment of cell sheets. Apart from PIPAAm, other biocompatible thermoresponsive materials, such as cellulose hydrogels, have also been applied in cell sheet generation [169, 170].

2.3.2.2. Light-based cell sheet generation. Light-based cell sheet technology refers to detaching cell sheets by changing the surface properties via light irradiation (figure 5(b)-ii). For example, Hong *et al* irradiated the titanium dioxide (TiO_2) nanodot films with 365 nm UV light to grant it superhydrophilicity, which made the cultured cells detach as a cell sheet [171]. Since then, TiO_2 has become the one of most widely used materials for light-based cell sheet generation. However, UV exposure may cause potential damage to cells during the

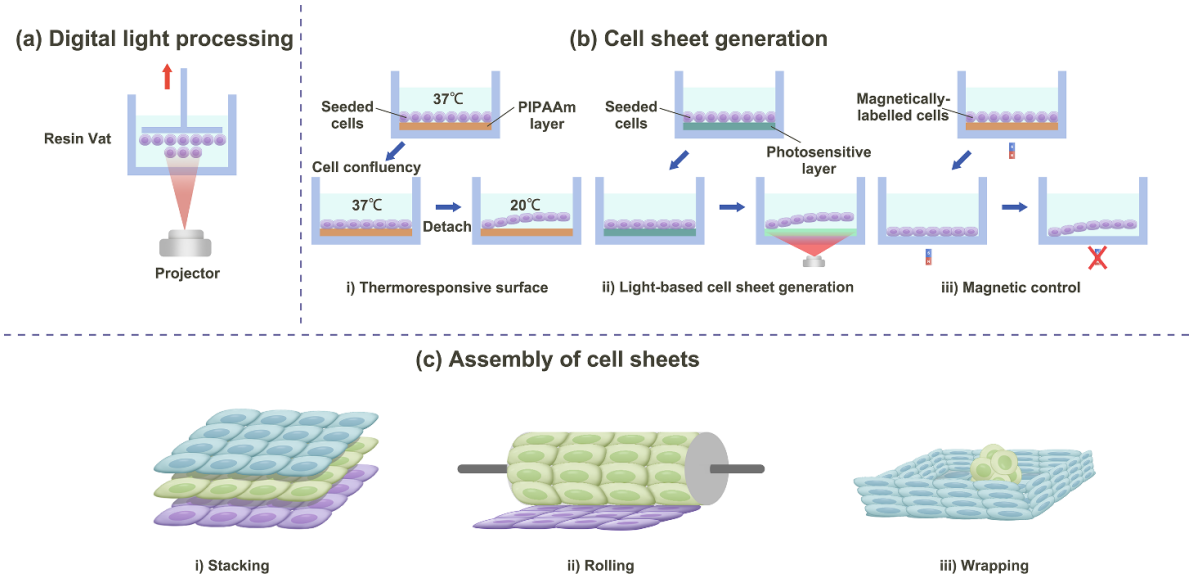

Figure 5. Schematic of enabling techniques for 2D single-cell building blocks manipulation. (a) Digital light processing applies the projector for illumination to crosslink a layer of photocurable ink and then the platform moves upward for next layer fabricating. (b) Representative techniques for cell sheet generation with two common steps: cell confluency and cell sheet detach. (c) High-order structures can be fabricated by orderly assembling cell sheets.

separation, so it is important to minimize the light dose. Wang *et al* incorporated the carbon quantum dots as a sensitizer into TiO_2 films and managed to shorten the exposure time from 20 min to 5 min for cell detachment [172]. The carbon quantum dots sensitization helped increase negative charge and caused changes in the secondary structure of adsorbed protein molecules. In other studies, researchers have tried visible and near-infrared light with lower energy to protect cells. For example, Wang *et al* applied the photovoltaic effect of silicon wafers under visible-light illumination to accumulate sufficient charge on the surface where the electrostatic repulsion forces removed the cell sheets [173]. In another work, Kim *et al* treated a collagen-coated layer with near-infrared light to induce the unfolding of collagen triple helices via a photothermal effect, leading to cell detachment [174]. More light-induced mechanisms can be used for cell detachment, including wettability transition. The ECM dissociation, and reactive oxygen species (ROS). For example, Koo *et al* fabricated a light-sensitive hematoporphyrin-polyketone film which could produce ROS under green light (510 nm) irradiation for cell detachment [175, 176]. By co-culturing with a fibrin gel substrate, the resultant detachment of cell sheets from the hematoporphyrin-polyketone film can transfer to the fibrin gel substrate. The authors also mentioned that long-term exposure to high-level ROS can cause damage to cells and DNA [177]. Overall, compared to other techniques, the light-based technique shows advantages in selective detachment of cells without cell labelling, but the effects of photosensitive materials and light on cells remain concern.

2.3.2.3. Magnetic control for cell sheet generation. The magnetic field can be used to generate and detach cell sheets if cells perform magnetic properties (figure 5(b)-iii), which can be achieved by labelling cells with magnetic Fe_3O_4 nanoparticles [178] and magnetite cationic liposomes [179]. Due to the magnetic attraction, cells can distribute well on a non-adhesive surface under the magnetic field. In this manner, Ito *et al* set a magnet below the low-adhesion cell culture dish where the labeled cells got attracted and form junctions with each other. Then generated cell sheets were easily detached from the culture dish after removing the magnet [30]. Insufficient magnetic force might result in cell clusters or vertical aggregation of cells, thus the magnetic parameter needed to be carefully optimized to achieve a monolayer of cell sheet [180]. Different from other cell sheet fabrication techniques, the magnetic control approach usually exhibits fast detachment of cell sheets and does not need a specific solution or surface modification for the detachment. Despite these advantages, it remains concerns for the safety and removal of magnetic labelling of cells [30, 178, 181–183]. For example, oxidative stress was implicated as one factor to damage vascular endothelial cells, and polymeric antioxidant bind to endothelial cells can protect against the cytotoxicity from iron oxide [184]. Together, further investigations are needed to better understand the influences of magnetic particles before turning to clinical applications.

2.3.2.4. Other techniques for cell sheet generation. Cell sheets can also be obtained using cell scrapers or tweezers to mechanically detach the confluent cell monolayer from the substrate [185–188]. This is an operator-dependent approach, and the generated cell sheets are usually multilayered [187]. Moreover, mechanical forces might damage the integrity of cell membranes [189]. To address these problems, ECM components such as fibrin gel can be added as a substrate of the cell sheet in advance [190].

Electrochemical desorption is another available approach for cell sheet detachment. Inaba *et al* grafted cell-adhesive peptides on an alkanethiol-coated gold surface via covalent bonding, which allowed for cell attachment and monolayer

formation [191]. Then the formed cell sheet can be obtained by separating the alkanethiol layer from the gold surface with electrical stimulation. To alleviate the potential side effects (e.g. cytotoxicity and inflammatory reaction) induced by the alkanethiol layer, Enomoto *et al* used the biodegradable oligopeptide to replace the alkanethiol and separated nearly 90% of cells in 3 min [192]. Additionally, the coated layer can be modified to obtain dynamic modulation of cell adhesion with electrochemical potentials. In this manner, Zhang *et al* succeed in modulating the accessibility to RGD via the switch of positive (RGD exposed) and negative potentials (RGD concealed) to control cell adhesion [193].

Ultrasonic vibration is another technique without the need for pre-treatment of culture substrate to detach cells [194]. Kurashina *et al* found that the acoustic pressure applied on cells and the resultant sloshing media induced by the intermittent travelling wave were the main factors for cell detachment [194]. And cell detachment will be limited in serum medium where the adhesion proteins prevent the cells from detaching. Further, Imashiro *et al* managed to detach the confluent mouse myoblasts monolayer cultured on a plastic surface via ultrasonic vibration induced by a longitudinal resonance from a Langevin transducer, and this method allowed cell detachment in the serum medium [195].

2.3.2.5. Assembly of cell sheets. Stacking is widely used to assemble 2D cell sheets with a sequential packing process [185, 196, 197] (figure 5(c)-i). Although the monolayer cell sheet can be manipulated and stacked by a simple pipetting method [198, 199], the 2D cell sheets are likely to deform because of the absence of material support. Therefore, Okano *et al* established a manipulator with a gelatin-coating surface to glue cell sheets and stack them layer by layer [200, 201]. This method showed advantages in preventing the shrinkage of cell sheets and was able to recycle the assembled cell sheets by dissolving the gelatin via heating. Later, the gelatin was replaced by the fibrin gel which served as supporting ECM and may enhance the mechanical property of cell sheets for implantation [202, 203]. These hydrogel manipulators enable the generation of heterogeneous tissue structures with up to ten layers of cell sheets. However, the current approach is a bit time-consuming (20–30 min per layer of cell sheet) as it needs to allow time for spontaneous cell adhesion [198]. As for the magnetic control technique, the stacking of cell sheets can be processed in both sheet-sheet assembling and sheet-cell assembling [182, 183, 204, 205]. Recently, Lu *et al* established a hamburger-like structure via stacking umbilical vein endothelial cells (UVECs) and dental pulp stem cells using the magnetic control technique [206]. Under the drive of a magnetic field, the magnetic-labelled cells can form a cell monolayer in 5 min while the lower cell layer would not be damaged. Thus, the magnetic field can accelerate the stacking process but additional culture time is still needed for the formation of cell junctions. Besides, the shape of the cell sheet can be tuned according to the magnetic field, which also enables the fabrication of heterogeneous tissue structures [207]. In general, stacking offers a reliable method for single-cell resolution assembly of multilayered tissues.

Rolling is a simple manner to curve the 2D cell sheets forming hollow or solid structures [186, 188, 208] (figure 5(c)-ii). For example, Germin *et al* managed to roll the smooth muscle cell sheet and fibroblast sheet with a polystyrene tube. They further made a sequential rolling of smooth muscle cell sheet and fibroblast sheet to form a tissue-engineered vascular adventitia, which exhibited considerable mechanical properties to sustain physiological pressures [186]. In another work, Kang *et al* constructed a biomimetic periosteum by rolling a cell sheet composited of human UVECs (HUVECs) and human mesenchymal stem cells (MSCs) and secondly rolling a cell sheet composited of osteogenic MSCs [188]. The self-adaption property of the cell sheet induced by its flexibility allows for adhesion on an irregular surface. In this manner, Jiang *et al* rolled the MSC sheets with a screw-shaped implant to enhance the osseointegration of the implants [209]. A manual rolling manner leads to poor accuracy in processing. In this regard, Othman *et al* developed an automated system that supported the rolling of multi-phase materials, including materials sheet and cell sheet [210]. However, this automated system required an additional substrate (i.e. alginate hydrogel) to offer mechanical support for a cell sheet during the rolling process. Based on the rolling strategy, the cell sheet can wrap other objects to form a higher-order cellular structure [211] (figure 5(c)-iii). Recently, a novel self-fold strategy was developed by Ramadhan *et al* to fabricate a liver microtissue [212]. They controlled the degradation of the redox-responsive hydrogel by tuning the reductant concentration. This leads to the cell sheet's self-folding behavior during the detachment from the hydrogel. With this technique, they succeed in wrapping HUVECs, collagen beads and liver cell spheroids with a fibroblast sheet. In summary, the cell sheet rolling or wrapping provides a simple but versatile tool to generate tubular, spherical, and even irregular structures with heterogeneity.

To have a better overview of the characteristics of the above mentioned biofabrication technologies, we have provided a table as table 1.

3. Advances in the application of biofabrication strategies with single-cell resolution

3.1. In vitro *models*

3.1.1. Single cell analysis. Analysis of bulk cell population can only reflect the overall information. Considering the common heterogeneity in cell populations, single-cell analysis has emerged to identify the minor subpopulations that play critical roles. Various single-cell manipulation techniques have been used to deliver single cells for downstream analysis.

The isolation and identification of single cells have allowed for a precise understanding of disease diagnostics. The circulating tumor cells, which only make up a small proportion in the bloodstream (estimated lower than 1 cell per million leukocytes), plays a crucial role in the early diagnosis of tumorigenesis and study on its invasion and metastasis [218, 219]. For example, Deng *et al* managed to isolate and

Table 1. Characteristics of biofabrication technologies of building blocks with single-cell resolution.

Dimension of the building blocks	Biofabrication technologies	Potential hazards to cells during fabrication	Applications	Merit and demerit
0D	Interface barrier trapping	—	Pattern primary neurons for generating neural networks [16]; High-throughput single-cell platform for drug screening [18]; Pattern single bacteria for high-throughput analysis [24].	High cell viability as cells are absent during barrier fabrication; Poor exchange of nutrients for cell culture within enclosed stencil with thick structures; Difficult to detach the single-cell assembly from the barrier.
	Free single-cell trapping	Magnetic materials [29, 33] and magnetic field [37]; Joule heating and direct field interactions [41]; Laser power [48, 50]; Heating or cavitation effects from sound waves [54]; Aspiration force.	Pattern cells for angiogenesis study [35]; Pattern-specific single bacteria as micro detection tools [36]; Spatial single-cell control and analysis [53]; Construct a paracrine signaling network [62]; *In vitro* model for immune responses study [23].	Enable spatial movement of single cells; Magnetic fields enable parallel manipulation of single cells but the introduced magnetic label is difficult to remove; Acoustic trapping is free of particle labelling; Single-cell self-assembly is free of mechanical-induced damage but faces challenges in controlling the assembling process; Aspiration-based trapping can precisely position and assemble single cells but the single cell directly suffers from the suction.
	Jetting-based single-cell printing	Shear stress [6]; Heating or cavitation effects from sound waves [54]; Pulse impact onto the substrate	Single cell patterning [86, 90]; Improve efficiency in single-cell cloning [97]; Construct cellular spheroids with heterogeneity [99].	High-throughout; Enable the generation of single-cell droplets but require real-time feedback systems to improve its efficiency; Difficult to use ink with high cell density and high viscosity.
	Droplet-based microfluidic technology	Flow stress	Single-cell droplets generation [105]; Niche modelling [106, 107].	High-throughout; Involvement of immiscible phase for droplet formation.
1D	Molding	Shear stress due to the perfusion into narrow structures	Fascicle-like tissue construct [115]; Fiber ink for cell culture [116].	Difficult to seed/perfuse single cells into molds with single-cell scale microstructure; Difficult to remove the single-cell assembly from the molds.

(Continued.)

Table 1. (Continued.)

	Extrusion bioprinting	Shear stress [121, 122]	Single-cell array printing [126]	Allow generation of customized fibers according to the shape of pre-set nozzles; High-viscosity ink limits the nozzle's diameter down to cell size for single-cell printing; Low-viscosity ink leads to unstable generation of single-cell fibers due to cell aggregation and sedimentation.
	Electrospinning and Electrowriting	Electric current [131]; Dehydration	3D cellular constructs for guided cell orientation [140]; 3D cellular constructs [143]; 3D cellular hybrid scaffolds with multiple scales [144, 145]; Hierarchical scaffold for skeletal muscle tissue engineering [146].	Enable processing of cell-laden ink to generate single-cell fibers; Difficult to generate large-scale architectures due to the weak mechanical properties of microfibrous structures.
	Wet spinning and Microfluidic spinning	Shear stress from the micronozzles	Guide neurite elongation [154]	Free of impact from electric fields and dehydration; Highly dependent on the rapid crosslinking mechanism.
2D	Digital light processing	Light irradiation; Cytotoxcity of photoinitiator and photoabsorbor	Microarchitecture construct for prevascularized tissue formation [160]	Rapid fabrication due to the use of patterning light for crosslinking; Difficult to generate heterogeneous structures with multi-materials; Limited to photosensitive materials; Cell-induced light scattering effect lowers the printing resolution.
	Cell sheet techniques	Light irradiation [171]; Reactive oxygen species for detachment [176]; Magnetic materials and magnetic field [180–183]; Mechanical damage from manual operation [188]; Ultrasonic vibration [193, 194].	Cardiac tissue engineering [197]; Microvascular-like networks pattern [199]; Prevascularized multi-layer myoblast sheet constructs [202]; Prevascularized stem cell microtissue [205]; Hepatocellular carcinoma spheroids [211].	Enable to generate cell sheets with the tight junction of cells; Enable stacking, rolling, and wrapping for assembling; Magnetic fields facilitate cell sheet formation but the magnetic label is difficult to remove; Difficult to control the cell location during the heterogeneous cell sheet formation.

enrich the circulating tumor cells (colorectal cancer cells) from whole blood by an integrated microfluidic chip where two secreted proteins (IL-8 and VEGF) related to colorectal cancer were assayed to demonstrate the feasibility of subsequent single-cell secretome analysis [220]. In another example, Armbrecht *et al* isolated the circulating tumor cells from whole

blood with more than 95% efficiencies by trapping single cells with functionalized magnetic beads [221]. The co-culture enabled the beads to capture the secreted protein from the cells, and the obtained data of epithelial adhesion molecule, human epidermal growth factor receptor 2 showed a sensitivity at the single-cell level. Additionally, the detection with single-cell sensitivity can also be visualized. Friedlander *et al* used a volumetric bar chart chip to quantify the oxygen generated by the reaction between hydrogen peroxide and a single targeted cell labeled with Pt nanoparticles [222] (see figure 6(a)). Moreover, high throughput characteristics grant single-cell assay the capacity of drug screening. Sadoun *et al* established a microfluidic single-cell device that can trap more than 2000 single cells at once for drug screening [223]. They further evaluated the feasible screening of targeted drugs by inhibiting the single-cell clone formation of cancer cell lines (e.g. MDA-MB-231) with specific agents (e.g. thiostrepton). These single-cell microarrays potentially enable single-cell analysis in a large scale. Xu *et al* used the patterned microarray chip to trap the single HeLa cells and monitor their activities including proliferation cycle, response to drug resistance and esterase activity dynamics for high-throughput screening [224].

Cell secretions are usually important regulators in the cellular microenvironment. Apart from disease diagnostics, single-cell analysis can be used to further study the differences induced by cell heterogeneity within the genetically identical cell population. Peng *et al* established a single-cell-laden environment where the secreted proteins can be captured for immunoassay without extraction [214]. This method showed high feasibility in analyzing low abundance essential secretions of a single cell, such as interleukin-6, interleukin-8, and monocyte chemoattractant protein-1, maintaining a high throughput screening speed (6000 cell h^{-1}) and secretion heterogeneity in these cytokines from individual cells was provided in this work. Due to the possible differences within the same population of cells, single-cell analysis becomes more important in specific scenarios at the single-cell level. Assisted reproduction technologies are a typical application where sperm selection is vital for successful fertilization. Von Erlach *et al* evaluated the single sperm from different aspects including cell viability, chromosomal content and acrosome state [225]. However, the contamination introduced in the analysis process limits the recycling of the target cells for downstream applications. In this regard, non-invasive and non-label techniques such as Raman spectroscopy and impedance detection may be a desiderate strategy to alleviate the potential influence on target cells in single-cell analysis.

3.1.2. Cellular and tissue models. The cell response to the signals from the external environment and cellular receptors can be regulated by external cues such as mechanical stress, electric signals, chemical exposure, or topographical cues. Cellular models with single-cell resolution enable a deeper vision to study the specific relationship between cells and the external environment. For example, Yao *et al* verified the specific immobilized function of CD45 antibody for T cells by selectively attaching the cells to single-cell scale spots coating with different adhesion molecules (e.g. bovine serum albumin, fibronectin, CD45 or CD43 antibody) [226]. Using atomic force microscopy and optical tracking of calcium fluxes, they further demonstrated the negligible influences of CD45 immobilization on activation and calcium reaction.

The topographical cues can also regulate cellular behavior at the single-cell level. Wang *et al* cultured single Schwann cells on the laminin patterns with different aspect ratios to reveal that the cell with elongated nuclei can upregulate the c-Jun expression, which is a remark of nerve repairing [215]. In another example, Lim *et al* used the cell-adhesion pattern with different geometric shapes to alter the morphology of a single MSC [227]. They found that the anisotropy of a single cell influenced the fate of its differentiation, which induced circular cells and anisotropic cells more likely to adipogenic differentiation and osteogenic differentiation, respectively (figure 6(b)). The geometry-dependent cytoskeletal contractility modulated the plasma membrane order by altering the abundance of lipid rafts and caveolae, which guided MSCs differentiation [228]. Apart from stem cells, the phenomenon of topographical cues in regulation exists in other cells such as cancer cells and adult cells. With the assistance of single-cell models, Chen *et al* managed to study the relation between cell spreading area and their proliferation behavior, and found two critical spreading areas of cells for proliferation (e.g. confined and free proliferation) in MSCs, Hela cell, and fibroblast cells, respectively [216]. The resultant differences in cytoskeletal structures induced by the geometric cues may lead to different cellular behavior. To study the influences of cytoskeletal structures on cellular uptake and DNA synthesis, Deng *et al* fabricated the array with single-cell scale micropatterns via selective surface modification and seeded the single cells onto the different micropatterns coated with fibronectin [229]. They found that the cellular uptake and DNA synthesis was improved in the larger spreading area and higher aspect ratio pattern, which may contribute to the transfection efficiency of MSCs (figure 6(c)).

The response to the external environment is highly related to the inherent properties of cells. Therefore, different cellular behaviors can be used to distinguish the cells. For example, Schmitz *et al* found that the benign breast cells seeded on the channels (with 10 μm depth) spread across channels to form cell sheets whereas the metastatic breast cancer cells remained spaced from each other [217]. However, apart from the identification between normal cells and cancer cells, the single-cell model can be used to recognize the migrating cell subpopulation which is curial to studying tumor metastasis. Armbrecht *et al* established a mimicking lymphatic capillary to distinguish the migrating breast cancer cells and low-migrating breast cancer cells based on their morphology of migrating the channel (figure 6(d)) [230].

The heterogeneity in cell behavior can cause unpredictable results even within a genetically identical population. To obtain sufficient data on the cell behavior of these single cells for statistical analysis, high throughput parallel experiments are important. Recently, Abate *et al* developed a multi-channel cultivation platform for the parallel culture of single

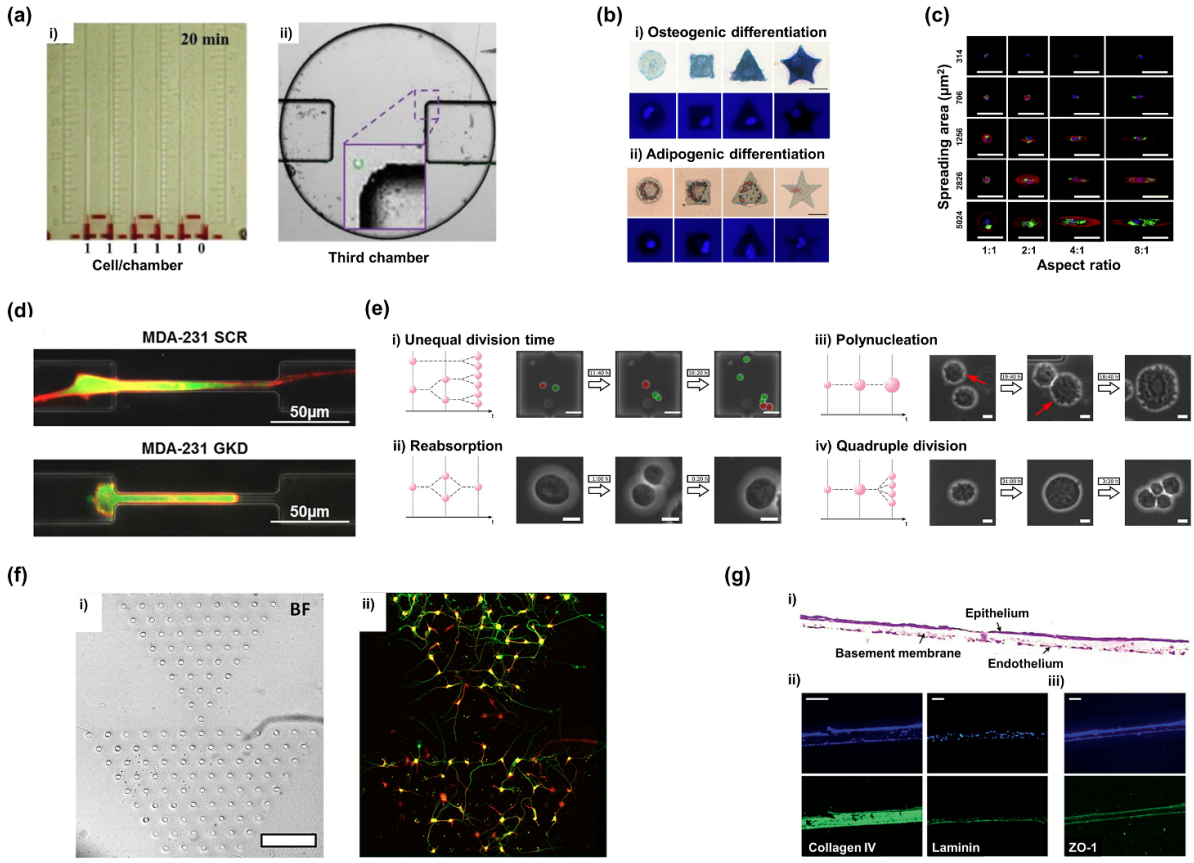

Figure 6. Examples of *in vitro* models with single-cell resolution. (a) Performance of Visual-Chip for detection of a single cell (i) and the image of the containing cell under the microscope (ii). [213] John Wiley & Sons. © 2019 WILEY-VCH Verlag GmbH & Co. KGaA, Weinheim. (b) Optical images (upper rows) of MSCs after (i) osteogenic differentiation and (ii) adipogenic differentiation, respectively. The fluorescent images (lower rows) with cellular nuclei labeled by DAPI illustrated individual cells with different morphology. Scale bar: 25 μm. Reprinted from [214], Copyright (2011), with permission from Elsevier. (c) Fluorescent images of human MSCs with different sizes and aspect ratios after uptake of cationic-modified microspheres (green). Actin filaments and nuclei are stained red and blue, respectively. Scale bar: 100 μm. Reproduced from [215] with permission from the Royal Society of Chemistry. (d) Migration behavior of MDA-MB-231 cells in the 6 μm $\times$ 10 μm capillary. The migrating cell (SCR) formed a stable and long stress fiber to migrate through the choke point, while the low-migrating cell (GKD) squeezed into the choke point. The green fluorescence proteins were expressed by cells and the F-actin fibers are labeled with red fluorescence protein. Reproduced from [216], with permission from Springer Nature. (e) Cell heterogeneity during mammalian single-cell cultivation. (i) Genetically identical cells with different doubling time. (ii) Reabsorption after cell division. (iii) Polynuclear cells (red arrow) induced by the absence of cell division. (iv) Quadruple division of one cell. Scale bar: (i) 50 μm; (ii), (iii), (iv) 10 μm. [217] John Wiley & Sons. © 2020 The Authors. Biotechnology and Bioengineering published by Wiley Periodicals LLC. (f) Optical image of the pattern with diode array for cell culture (i). And the fluorescent image of neurons stained for Tau-1 (green) and MAP2 (red) (ii). Scale bar: 200 μm. Reproduced from [16], with permission from Springer Nature. (g) The cross-sectional image of engineered alveolar barrier stained with hematoxylin & eosin (i). The collagen IV and laminin resulted from cell-ECM interaction existed in the basement membrane (ii). The tight junction protein ZO-1 illustrated a solid intercellular connection (iii). The nuclei in (ii), and (iii) were stained blue. Scale bar: (i) 20 μm; (ii), (iii) 50 μm. [5] John Wiley & Sons. © 2021 The Authors. Advanced Science published by Wiley-VCH GmbH.

suspension cells to detect the heterogeneous growth and division behavior among the Chinese hamster ovary cell population via a single-cell culture manner (figure 6(e)) [213]. In another example, Lin *et al* applied jetting-based printing to generate an MCF-7 cell array to study the effect of adenosine triphosphate (ATP) on single-cell proliferation [231].

In vitro cellular models with single-cell resolution are also beneficial for understanding intercellular interactions, which are crucial for fundamental and clinical applications. For example, Li *et al* established a neuro pattern where the single cell was trapped within a hole but it can spread and form a connection with others to study the interaction of neurons in a hierarchical [16]. In this work, the patterned single neuro can grow and form a diode-like neural network where the neuronal activities can be tracked and recorded along with calcium imaging (figure 6(f)). Insufficient and misdirected axonal outgrowth can lead to failure of the reinnervation [232]. To study the role of physical cues in stem cell differentiation, Solanki *et al* established different cellular models with squares, stripes, and grids patterns to study their differentiation, and they found that the neural stem cells in a grids pattern were more likely to differentiate to neurons even without adding soluble factors [233]. But little neural stem cells differentiated in both the unpatterned group and the group with pattern dimensions

above 50 μm. That means the cellular interactions are not only referred to the physical cues but also to the scale of these cues, which suggests the necessity of single-cell *in vitro* models. The advances in single-cell biofabrication techniques also enable the generation of tissue models with precise architectures. For example, Kang *et al* recapitulated a three-layered alveolar barrier model with a thickness of almost 10 μm [5]. The monolayer of human alveolar-related cells was created by inkjet printing and three overlapped monolayers were printed orderly to form the 3D alveolar barrier model. The engineered model possessed a high level of type IV collagen synthesized inside the basement membrane and expressed laminins along the boundary of the basement membrane in contact with the endothelium and epithelium (figure 6(g)). Compared to the unorganized model, tight junction protein ZO-1 and high expression of pulmonary surfactant markers (SP-A and SP-B) were found in the bioprinted models. These results implied the tight junction formation of the alveolar barrier and its physiological functions of barrier properties, which enabled the model to take an immune response to the influenza A virus. Together, cellular and tissue models with single-cell features allow for the precise analysis of cell response and behavior. These models serve as supplementary tools to cover the shortage of population-based cellular models in mimicking the native microenvironment.

3.2. Regenerative medicine

3.2.1. Aligned tissue constructs. The assembling of aligned structures of cell filaments with single-cell scale into fibrous bundles is a promising strategy for the precise fabrication of anisotropic tissues, such as nerves, muscles and blood vessels. For example, Patil *et al* orthogonally stamped the fibronectin solution on alginate microfibers (20 μm in width) to generate adhering area for guiding the cell direction [234]. The patterned fibers used as a scaffold for cell strand assembly allow for resembling the natural muscle structure with orientation (figure 7(a)). The single-cell biofabrication techniques enable more accurate controllability of cells to construct fine architectures where cell junctions would be limited to the desirable direction for alignment. In contrast, the cells in a population-based engineered structure may lead to a low organization due to the unwanted interaction between surrounding cells [141]. As shown in figure 7(b), the 3D construction composited of single-cell fibers printed by electrohydrodynamic bioprinting can better guide cell orientation. In another study, Yeo *et al* fabricated an aligned structure by direct electrospinning the UVECs-laden ink, which contributed to the myoblast formation of the myoblasts seeded onto the aligned constructs [147]. Compared to the cell seeding group, the cell-laden electrospinning group showed better performance in promoting vessel development. The myoblast seeded to the cell-laden electrospinning scaffold showed enhanced myogenic maturation. Very recently, Yeo *et al* electrospun the smooth muscle cells onto the PCL fibrous membrane to form an aligned cellular patch for esophageal regeneration [238]. After implantation, the engineered patch facilitated epithelial cell recruitment for better vascularization, improving esophageal muscle regeneration. Another common strategy for generating single-cell scale alignment is creating microchannels, particularly for constructing blood capillaries. For example, Rayner *et al* used multiphoton ablation techniques to construct 3D microvascular structures in collagen hydrogels as engineered microvascular tissues to recapitulate glomeruli where the HUVECs migrated into the narrow lumens then endothelialized under gravity-driven flow (figure 7(c)) [235]. Due to the small size of the channels, it is challenging to perfuse the cell solution to the microchannels [115]. Overall, the assembly of single-cell scale building blocks shows advantages in generating heterogeneous structures in single-cell resolution as well as guiding the cells to forming aligned structures. However, the assembling of building blocks with single-cell resolution usually induces weak mechanical properties and time-consuming processing, which limits its use in producing large-scale products for regenerative medicine applications. Advances in manipulating cellular filaments and co-culturing multiple cells are needed in building sophisticated heterogeneous structures.

3.2.2. Mono/multilayer tissue constructs. Tissues with multilayer architectures require the construction of lamellar structures with single-cell precision. Cell sheet technology can obtain a confluent layer of cells as the basic unit to assemble a multilayer tissue while preserving the intercellular matrix as well as connections, providing an implant with a similar cell density to the natural tissue [198]. Compared to the dissociated cell injection, the cell sheet is more suitable for transplant with less cell loss. Further, the scaffold-free cell sheet assembly can reduce the potential inflammatory reactions caused by introducing scaffolds, while providing a method for tissue engineering vascularization.

Corneal is a multi-layer structure, compositing different thin cellular lamina such as epithelium and epithelial. The use of cell sheet technology in corneal repair is natural due to its superiority of cellular lamina generation with single-cell resolution. Epithelial cells can be extracted from the patient's healthy cornea or mouth and cultured to prepare cell sheets that can be transplanted directly onto the injured cornea without sutures [239]. Epithelial cell sheets show a low immune response and ideal grafting results in corneal transplants [240]. The endothelium has little capacity for cell proliferation *in vivo* but exhibits complex barrier and pump function [241], making it difficult to repair. For this matter, Ide *et al* managed to introduce endothelial cell sheets for repairing the corneal endothelium [242]. The cell sheet exhibited similar characteristics to the *in vivo* structure such as a hexagonal shape of cells and microvilli. In another example, Sumide *et al* fabricated a human corneal endothelial cell sheet with single-cell layer and then grafted it to the rabbit model [236]. The Xenograft transplantation results showed that the implanted endothelial cell sheet remained a laminar structure beneath the corneal stroma and possibly functioned to transport ions from the corneal stroma (figure 7(d)). The cell sheets can also be delivered by injection. For example, Jia *et al* developed an injection method to transplant corneal endothelial cell sheets

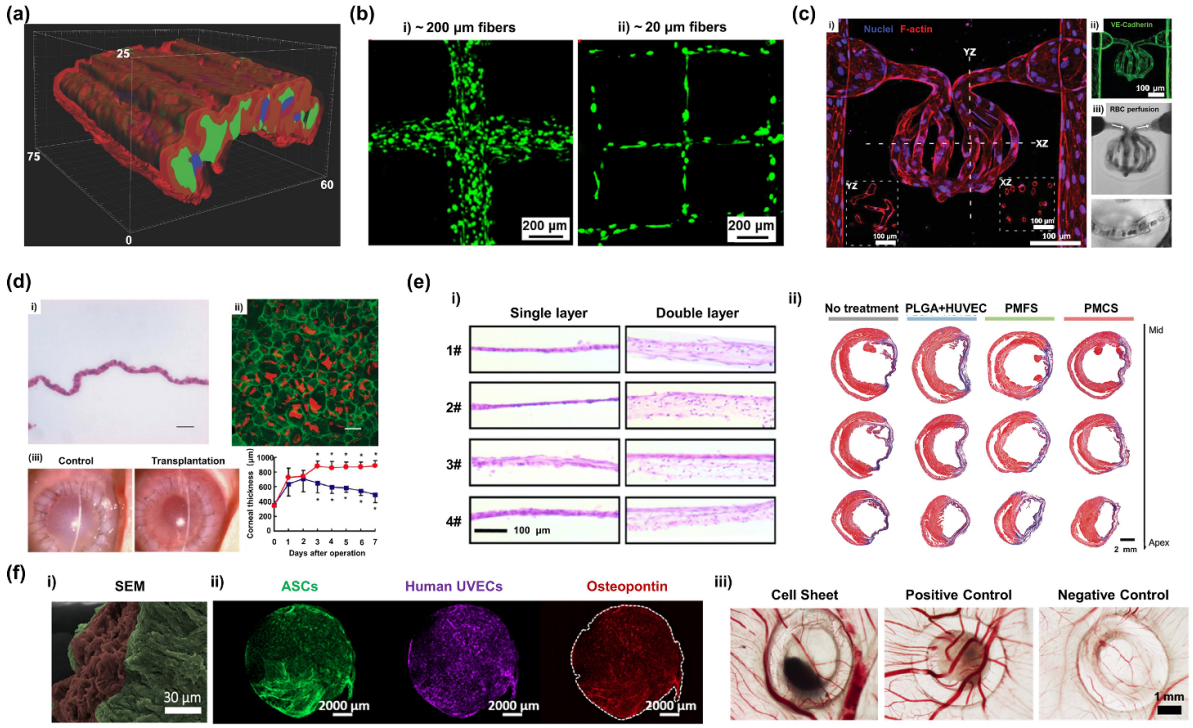

Figure 7. Applications of products with single-cell resolution for regenerative medicine. (a) 3D image of a section of the muscle-like microfibers where cells are stained for nuclei (blue), fibronectin (red), and F-actin (green). [234] John Wiley & Sons. © 2016 WILEY-VCH Verlag GmbH & Co. KGaA, Weinheim. (b) Printed C2C12 constructs composited of (i) $\sim$200 μm fibers obtained by conventional extrusion bioprinting and (ii) $\sim$20 μm fibers by electrohydrodynamic bioprinting, respectively. The live staining images of cell structures were obtained after >24 h culture. Reproduced from [141], with permission from Springer Nature. (c) Glomerular structure containing 3D cellularized microvessels. (i) 3D images of glomerulus with inset cross-sectional views of the YZ and XZ plane, respectively; (ii) VE-cadherin staining illustrated the tight junction of the endothelial monolayer; (iii) Red blood cells perfusion with single-cell transit (bottom) illustrated microvessels' function. [235] John Wiley & Sons. © 2021 The Authors. Advanced Healthcare Materials published by Wiley-VCH GmbH. (d) The harvested cell sheet with a continuous monolayer was illustrated by Hematoxylin and Eosin staining (i). Anti-Na+, K+-ATPase antibody (green) and propidium iodide (red) staining results showed that a certain pump function of corneal endothelial cell sheets resulted from the distribution of Na+, K+-ATPase pump (ii). Slit lamp microscopy of the rabbit model from the control group (red) and transplantation group (blue) after 7 day surgery and measure of their average corneal thickness after transplantation both illustrated that cell sheets transplantation helped corneas reduce thickness, decrease swelling and improve transparency (iii). Scale bar: (i), (ii) 20 μm. [236] John Wiley & Sons. © FASEB. (e) Characterization of prevascularized, multiple-layered cell sheets. (i) H&E staining at cross-section of single- or double-layer cell sheets of different groups after 7 day culture; (ii) Images of Masson's trichrome-stained infarcted hearts at 8 weeks after implantation from different groups, i.e. no treatment, PLGA membranes seeded with endothelial cells (PLGA + HUVEC), prevascularized multilayered fibroblast sheets (PMFS) and prevascularized multilayered cardiac reprogrammed cells sheets (PMSC). Reduction in the fibrotic area was found in the PMCS group. Reproduced from [237] with permission from the Royal Society of Chemistry. (f) Scanning electron micrographs of the triple-layer cell sheets containing UVECs (red) and ASCs (green) (i). Immunofluorescence of ASCs (green), UVECs (purple) and osteopontin (red) in cell sheets cultured for 21 d in basal media without osteogenic factors showed osteogenesis phenomenon (ii). Images of the newly formed vessels in chick chorioallantoic membrane assay from cell sheet, basic fibroblast growth factor solution (positive control) and phosphate buffer solution (negative control) illustrated the *in vivo* angiogenic potential of the cell sheets (iii). Reprinted from [183], Copyright (2020), with permission from Elsevier.

into the anterior chamber. The *in vivo* experiment results showed that the corneal clarity and thickness recovered more rapidly in the cell sheet injection group than that in the cell suspension injection group [243]. This difference may be related to the adhesion and tight junction of cells in cell sheets.

Similarly, cell sheet transplantation has demonstrated a better repair outcome compared to intra-myocardial injection of cell suspensions for myocardial repair [244]. Different cell types, including skeletal muscle cells, MSCs, adipocytes, and cardiomyocytes from newborn rats, have been used in the cell sheet technique for repairing myocardial tissue [245]. Early in 2012, Sawa *et al* reported clinical transplantation of autologous myoblast sheets. The results showed that no arrhythmia appeared in the patients, enabling the discontinued use of a left ventricular assist system [246]. Later, Tanaka *et al* implanted a hypoxia-pretreated autologous bone MSCs sheet into a rabbit model and demonstrated an ameliorative effect on cardiac infarction [247]. These works demonstrated the potential of cell sheets in cardiac repair. Based on these inspiring experiences, the researchers further introduced the induced PSCs in cell sheets to address the issue of the cell source of myocardial tissue. Kawamura *et al* prepared cell sheets using human-induced PSCs derived from cardiomyocytes (hiPS-CMs) and combined them with omental flaps for ischemic cardiomyopathy treatment trials in pigs [248]. The results showed that hiPS-CMs improve cardiac function in ischemic cardiomyopathy by secreting multiple angiogenic factors [249], while the combination of omental flaps improves the survival

rate of hiPS-CM cell sheets after transplantation. In summary, the cell sheet can be assembled to form an implant for cellular therapy, but the limited vascularization after transplantation is a concern [250]. A promising trend to enhance the clinical effect of the thick assembly of cell sheets is the prevascularization of the multilayer cell sheets. Song *et al* laid out the cell sheets layer by layer and prevascularized them by embedding endothelial cells between the layers [237]. Rat transplantation experiments showed that the prevascularized cell sheets reduced the area of fibrosis resulting from myocardial infarction and promoted the recovery of cardiac function (figure 7(e)).

Traditional scaffold-based methods for bone repair face limitations such as dependence on scaffold materials and insufficient vascularization. Multilayer cell sheet assembly provides a promising solution. Shimizu *et al* performed bone-repairing experiments on rats by injecting osteogenic cell sheets made from rat bone marrow stromal cells [251]. A hard callus induced by the recorticalization was found after 12 weeks, demonstrating the possibility of cell sheet assembly in promoting bone regeneration. Apart from bone repairing, these cell sheet assembly also has great potential in cartilage regeneration. Zhou *et al* implanted human rib-derived chondrocyte sheets into nude mice [252]. The newly formed cartilage in the harvested cartilage discs possessed similar morphology and ECM components to native rib cartilage. Vascularization is key to bone tissue repair. Necrosis resulting from a lack of vascular tissue limits the regenerative size of bone tissue grafts. One solution is to assemble osteoblast sheets with vascular endothelial cell sheets as implants. The results of subcutaneous transplantation in nude mice validated the osteogenic and vascularizing ability of the hybrid cell sheet assembly [253]. Recently, Xu *et al* established a double-layer cell sheet composited of BMSCs-derived endothelial cells and BMSCs cell sheets for pre-vascularization [254]. After endothelial cells migrated and rearranged to form lumens, the cell sheets were then superimposed on BMSC-derived osteoblast sheets to generate a triple-layer cell sheet for bone regeneration. The pre-vascularized cell sheets exhibited enhanced bone tissue and vascular regeneration. In addition, the cell sheet assembly technique with single-cell precision can be applied to mimic the bilayer structure of the periosteum. Kang *et al* seeded HUVECs on undifferentiated hMSCs sheets to generate the fibrous layer, while cultured osteogenic hMSC sheets acted as the osteogenic layer [188]. The two cell sheets were combined orderly onto β-TCP scaffolds to form a periosteal implant. Nude mouse transplantation experiments demonstrated its role in promoting angiogenesis and osteogenesis.

In addition to the preservation of intercellular connections, the assembly of homogeneous or heterogeneous cell sheets is a greater advantage of the cell sheet techniques which enables to fabrication of mono/multi-layer cellular laminas at single-cell resolution. By assembling and pre-vascularizing multilayer cell sheets, thick tissue grafts with a vascular structure can be constructed *in vitro*. Sasagawa *et al* assembled HUVECs with myogenic cell sheets to fabricate a five-layer structure, in which endothelial cells formed connections through the layers, constructing capillary-like structures [202]. This pre-vascularization strategy is versatile in other tissue repairs. For example, Lee *et al* mixed endothelial cells and fibroblasts with a fibrin hydrogel solution to generate a pre-vascularized substrate in which the Keratinocytes were seeded and co-cultured to form mucosal cell sheets [255]. Compared to the skin graft, the cell sheets graft promoted wound closure and suppressed fibrotic features leading to scar tissue formation. The cell sheet assembly can also be applied to tissues with a cavity. For example, Chen *et al* transplanted a cellular assembly composited of smooth muscle cell sheets and endothelial progenitor cells for bladder repair [256–258]. Interestingly, these multilayer cell sheets assembly can achieve differentiation of stem cells via their interaction. In another study, Silva *et al* sandwiched HUVECs between two layers of adipose-derived stromal cells (ASCs) by magnetic forces [183]. In cooperation with the synergic interaction between UVECs and ASCs, the self-generation of growth factors and proteins facilitates osteogenesis in the cellular construct without additional osteogenic differentiation factors and its *in vivo* angiogenic potential was shown by embedding the cell sheet assembly into chick chorioallantoic membrane (figure 7(f)).

4. Concluding remarks and future perspectives

The generation and assembly of living building blocks are the two key steps for modular biofabrication with single-cell resolution. For 0D single-cell building blocks, some of the above-mentioned techniques have enabled the isolation from cell populations and the formation of 1D and 2D patterns. Specifically, the free single-cell trapping techniques offer spatial control of cells with single-cell resolution, whereas the regional field-based techniques (i.e. magnetic, dielectrophoretic, and acoustic fields) would need to confine the field to single-cell level for assembling heterogeneous cells. In contrast, the interface barrier trapping technique has limited control over single cells spatially. Combined with a mobile platform, aspiration trapping can be used to deposit single cells spatially, but its damage to cells remains unclear. The droplet-based microfluidic techniques can be incorporated with a sorting approach to improving the efficiency of generating single-cell droplets, which further enhances the manufacturing capacity of jetting-based bioprinting. For 1D single-cell building blocks assembling, the molding technique can generate intricate patterns with single-cell resolution, but fine filaments are usually used as substracts to attract cells to form 1D single-cell fibers on their surfaces. The emergence of suspension bioprinting makes it possible with printing low-viscosity bioinks (even the cell suspension), which might ease the shear impact on cells while printing single-cell fibers with a narrow nozzle. However, the possible cell aggregation and sedimentation with low-viscosity bioinks are likely to bring challenges to single-cell fibers deposition. Currently, electrospinning and electrowriting have been applied to fabricate patterns or structures made of single-cell fibers. By combining with other techniques (e.g. fused deposition techniques), hybrid cellular scaffolds with

multiscale features can be obtained. Wet spinning and microfluidic spinning offer an electric-free and mild processing method to generate 1D single-cell fibers that can be assembled to form 2D patterns or 3D cellular structures via weaving, reeling, knitting, and stacking techniques. For 2D single-cell building block assembling, digital light processing is a representative technique among light-based biofabrication techniques, which can generate customized 2D patterns or 3D structures. The cell-induced scattering of light should be well addressed for the fabrication with single-cell resolution. Cell sheet techniques provide a scaffold-free method to fabricate 2D cellular monolayer building blocks that can be further assembled via stacking, rolling and wrapping to form 3D structures. All the 0D (single-cell droplets), 1D (single-cell filaments), and 2D (single-cell sheets) building blocks can be used as modules to assemble higher-order patterns and architectures depending on the demands. According to the basic principle of geometry, 0D building blocks possesses the highest resolution in space, while it yields the lowest speed for scaling up (figure 2). Together, different building blocks might suit different scenario; 0D single-cell droplets can form heterogeneous microenvironment down to single-cell scale, while 1D single-cell filaments show superior performance on cell orienting and 2D single-cell sheets exhibit tight cell–cell junction.

Assembly of cellular building blocks with single-cell resolution is a promising strategy to recapitulate the natural living system where single-cell features are vital. Although early single-cell isolation and manipulation techniques were mostly used for high-throughput screening and single-cell analysis, the advantages of spatial assembly of single-cell units have been recently realized for cellular *in vitro* modeling and regenerative medicine applications. Differences in cellular behavior have been found between single-cell-resolution models and cell-population models, which are likely related to the inherent properties of cells and the biophysical cues (e.g. topological structure and extracellular matrix component). As for regenerative medicine, high-order heterogeneous structures can be engineered by assembling 0D single-cell building blocks but is merely possible for cell population assembly techniques. Nevertheless, these single-cell biofabrication technologies can also enable the fabrication of scaffold-free and high-density cellular structures by assembling 1D and 2D single-cell building blocks for tissue/organ repair.

Currently, single-cell printing [70, 72, 87] and assembly [23, 64] have already been achieved. However, the single-cell assembly strategy in recapitulating the complex architecture still faces some major challenges, such as the adhesion of the individual cells before fusion, the integration of the ECM, and the long processing time. Before completely reconstructing a large-scale tissue, microphysiological models may be more achievable for single-cell biofabrication strategies. Recently, organoids have attracted much attention as they can resemble the 3D structure, composition, and biological function of an organ to some extent [259]. Mostly, the formation of organoids relies on the self-assembly of stem cells [260], which may cause heterogeneity in organoids due to the unpredictable behavior of cell populations [261–263]. The assembly method has been used to generate organoids by directly assembling various types of cells spatially, which can form high-level organoids with mature functions [264] or large-scale [265]. Thus, in cooperation with single-cell analysis, screening and machine learning, the selective cells can be assembled to create the organoids, which seems an alternative method to improve their controllability, repeatability, and even functionality.

Satisfied mechanical property is a major challenge for cellular implants fabricated by single-cell biofabrication techniques. Mostly, the living structures created by single-cell biofabrication fail to meet the requirements of implantation or collapse after implantation due to their delicate construction without sufficient support from materials. The cell sheet techniques can be used to create transplantable structures, but these engineered implants are still difficult to maintain construction *in vivo*. Therefore, it is an alternative to fabricating heterogeneous structures by means of assembly strategies that use cell-population or biomaterial blocks to generate mechanical supporting components while the single-cell blocks are used to resemble fine structures with single-cell distribution. On the other hand, efficiency is another concern with single-cell-resolution biofabrication. In modular assembly biofabrication, the fabrication speed is highly related to the dimension and scale of the assembling units. Thus, it is helpful to select the proper single-cell building blocks for specific uses, considering the balance between the resolution and fabricating efficiency. For the techniques requiring single-cell building block catching (e.g. aspiration-based trapping), reducing the sample loading time and continuous deposition can dramatically improve the efficiency. Besides, for the techniques with feedback systems for real-time monitoring, an optimized algorithm is beneficial to shorten the computing time. The hybrid assembly strategy that combined cell-population-based blocks and single-cell-based blocks is also promising to improve the efficiency of single-cell biofabrication for large-scale object manufacturing.

In all, biofabrication with single-cell resolution greatly adds to the cell-population biofabrication to recapitulate the single-cell features. The combination of single-cell-feature building blocks and cell-population/biomaterial building blocks should advance the building of higher-order heterostructures with both physicochemical and biological features, contributing to the engineering of complex tissues.

Acknowledgments

The authors declare no conflict of interest. The authors acknowledge the financial support from the National Natural Science Foundation of China (No. 52105306, 32211530075) and New Faculty Start-up Funding provided by Tsinghua University (012-53330200421).

ORCID iD

Liliang Ouyang https://orcid.org/0000-0003-4177-8698

References

[1] Jakab K, Norotte C, Marga F, Murphy K, Vunjak-Novakovic G and Forgacs G 2010 Tissue engineering by self-assembly and bio-printing of living cells *Biofabrication* **2** 022001

[2] Guven S, Chen P, Inci F, Tasoglu S, Erkmen B and Demirci U 2015 Multiscale assembly for tissue engineering and regenerative medicine *Trends Biotechnol.* **33** 269–79

[3] Li J, Klughammer J, Farlik M, Penz T, Spittler A, Barbieux C, Berishvili E, Bock C and Kubicek S 2016 Single-cell transcriptomes reveal characteristic features of human pancreatic islet cell types *EMBO Rep.* **17** 178–87

[4] Mukund K and Subramaniam S 2020 Skeletal muscle: a review of molecular structure and function, in health and disease *WIREs Syst. Biol. Med.* **12** e1462

[5] Kang D, Park J A, Kim W, Kim S, Lee H R, Kim W J, Yoo J Y and Jung S 2021 All-inkjet-printed 3D alveolar barrier model with physiologically relevant microarchitecture *Adv. Sci.* **8** 2004990

[6] Li X D, Liu B X, Pei B, Chen J W, Zhou D Z, Peng J Y, Zhang X Z, Jia W and Xu T 2020 Inkjet bioprinting of biomaterials *Chem. Rev.* **120** 10793–833

[7] García Alonso D, Yu M C, Qu H J, Ma L and Shen F 2019 Advances in microfluidics-based technologies for single cell culture *Adv. Biosyst.* **3** 1900003

[8] Bertassoni L E 2022 Bioprinting of complex multicellular organs with advanced functionality—recent progress and challenges ahead *Adv. Mater.* **34** 2101321

[9] Zandrini T, Florczak S, Levato R and Ovsianikov A 2023 Breaking the resolution limits of 3D bioprinting: future opportunities and present challenges *Trends Biotechnol.* **41** 604–14

[10] Zhou X H, Wu H, Wen H T and Zheng B 2022 Advances in single-cell printing *Micromachines* **13** 80

[11] Wang Z H, Lang B H, Qu Y M, Li L, Song Z X and Wang Z B 2019 Single-cell patterning technology for biological applications *Biomicrofluidics* **13** 061502

[12] Ouyang L L, Armstrong J P K, Salmeron-sanchez M and Stevens M M 2020 Assembling living building blocks to engineer complex tissues *Adv. Funct. Mater.* **30** 1909009

[13] Xing J Y, Liu N, Xu N N, Chen W J and Xing D M 2022 Engineering complex anisotropic scaffolds beyond simply uniaxial alignment for tissue engineering *Adv. Funct. Mater.* **32** 2110676

[14] Du K, Ding J J, Liu Y Y, Wathuthanthri I and Choi C H 2017 Stencil lithography for scalable micro- and nanomanufacturing *Micromachines* **8** 131

[15] Wu J B, Zhang M Y, Chen L Q, Yu V, Tin-Yum Wong J, Zhang X X, Qin J H and Wen W J 2011 Patterning cell using Si-stencil for high-throughput assay *RSC Adv.* **1** 746–50

[16] Li W, Xu Z, Huang J Z, Lin X D, Luo R C, Chen C H and Shi P 2014 NeuroArray: a universal interface for patterning and interrogating neural circuitry with single cell resolution *Sci. Rep.* **4** 4784

[17] Miranda I, Souza A, Sousa P, Ribeiro J, Castanheira E M S, Lima R and Minas G 2022 Properties and applications of PDMS for biomedical engineering: a review *J. Funct. Biomater.* **13** 2

[18] Huang L, Chen Y, Chen Y F and Wu H K 2015 Centrifugation-assisted single-cell trapping in a truncated cone-shaped microwell array chip for the real-time observation of cellular apoptosis *Anal. Chem.* **87** 12169–76

[19] Huang C K, Paylaga G J, Bupphathong S and Lin K H 2020 Spherical microwell arrays for studying single cells and microtissues in 3D confinement *Biofabrication* **12** 025016

[20] Liu C S, Liu J J, Gao D, Ding M Y and Lin J M 2010 Fabrication of microwell arrays based on two-dimensional ordered polystyrene microspheres for high-throughput single-cell analysis *Anal. Chem.* **82** 9418–24

[21] Zhang K, Chou C K, Xia X F, Hung M C and Qin L D 2014 Block-cell-printing for live single-cell printing *Proc. Natl Acad. Sci. USA* **111** 2948–53

[22] Stevens A J *et al* 2022 Programming multicellular assembly with synthetic cell adhesion molecules *Nature* **614** 144–52

[23] Todhunter M E, Jee N Y, Hughes A J, Coyle M C, Cerchiari A, Farlow J, Garbe J C, LaBarge M A, Desai T A and Gartner Z J 2015 Programmed synthesis of three-dimensional tissues *Nat. Methods* **12** 975–81

[24] Xu L P, Robert L, Ouyang Q, Taddei F, Chen Y, Lindner A B and Baigl D 2007 Microcontact printing of living bacteria arrays with cellular resolution *Nano Lett.* **7** 2068–72

[25] Bhujbal S V, Dekov M, Ottesen V, Dunker K, Lale R and Sletmoen M 2020 Effect of design geometry, exposure energy, cytophilic molecules, cell type and load in fabrication of single-cell arrays using micro-contact printing *Sci. Rep.* **10** 15213

[26] Wu H, Wu L, Zhou X H, Liu B S and Zheng B 2018 Patterning hydrophobic surfaces by negative microcontact printing and its applications *Small* **14** 1802128

[27] Colombo M, Carregal-Romero S, Casula M F, Gutiérrez L, Morales M P, Böhm I B, Heverhagen J T, Prosperi D and Parak W J 2012 Biological applications of magnetic nanoparticles *Chem. Soc. Rev.* **41** 4306–34

[28] Mattix B, Olsen T R, Gu Y, Casco M, Herbst A, Simionescu D T, Visconti R P, Kornev K G and Alexis F 2014 Biological magnetic cellular spheroids as building blocks for tissue engineering *Acta Biomater.* **10** 623–9

[29] Ino K, Ito A and Honda H 2007 Cell patterning using magnetite nanoparticles and magnetic force *Biotechnol. Bioeng.* **97** 1309–17

[30] Ito A, Hayashida M, Honda H, Hata K-I, Kagami H, Ueda M and Kobayashi T 2004 Construction and harvest of multilayered keratinocyte sheets using magnetite nanoparticles and magnetic force *Tissue Eng.* **10** 873–80

[31] Aermes C, Hayn A, Fischer T and Mierke C T 2020 Environmentally controlled magnetic nano-tweezer for living cells and extracellular matrices *Sci. Rep.* **10** 13453

[32] Tasoglu S, Yu C H, Gungordu H I, Guven S, Vural T and Demirci U 2014 Guided and magnetic self-assembly of tunable magnetoceptive gels *Nat. Commun.* **5** 4702

[33] Moncal K K, Yaman S and Durmus N G 2022 Levitational 3D bioassembly and density-based spatial coding of levitoids *Adv. Funct. Mater.* **32** 2204092

[34] Durmus N G, Tekin H C, Guven S, Sridhar K, Arslan Yildiz A, Calibasi G, Ghiran I, Davis R W, Steinmetz L M and Demirci U 2015 Magnetic levitation of single cells *Proc. Natl Acad. Sci. USA* **112** E3661–8

[35] Ino K, Okochi M and Honda H 2009 Application of magnetic force-based cell patterning for controlling cell–cell interactions in angiogenesis *Biotechnol. Bioeng.* **102** 882–90

[36] Pivetal J, Royet D, Ciuta G, Frenea-Robin M, Haddour N, Dempsey N M, Dumas-Bouchiat F and Simonet P 2015 Micro-magnet arrays for specific single bacterial cell positioning *J. Magn. Magn. Mater.* **380** 72–77

[37] Zablotskii V, Polyakova T, Lunov O and Dejneka A 2016 How a high-gradient magnetic field could affect cell life *Sci. Rep.* **6** 37407

[38] Hunt T P and Westervelt R M 2006 Dielectrophoresis tweezers for single cell manipulation *Biomed. Microdevices* **8** 227–30

[39] Weiss N G, Jones P V, Mahanti P, Chen K P, Taylor T J and Hayes M A 2011 Dielectrophoretic mobility

determination in DC insulator-based dielectrophoresis *Electrophoresis* **32** 2292–7
[40] Albrecht D R, Sah R L and Bhatia S N 2004 Geometric and material determinants of patterning efficiency by dielectrophoresis *Biophys. J.* **87** 2131–47
[41] Voldman J 2006 Electrical forces for microscale cell manipulation *Annu. Rev. Biomed. Eng.* **8** 425–54
[42] Gray D S, Tan J L, Voldman J and Chen C S 2004 Dielectrophoretic registration of living cells to a microelectrode array *Biosens. Bioelectron.* **19** 1765–74
[43] Yang Y J, Mao Y F, Shin K S, Chui C O and Chiou P Y 2016 Self-locking optoelectronic tweezers for single-cell and microparticle manipulation across a large area in high conductivity media *Sci. Rep.* **6** 22630
[44] Polimeno P *et al* 2018 Optical tweezers and their applications *J. Quant. Spectrosc. Radiat. Transfer* **218** 131–50
[45] Zhang H and Liu K K 2008 Optical tweezers for single cells *J. R. Soc. Interface* **5** 671–90
[46] Favre-Bulle I A, Stilgoe A B, Rubinsztein-Dunlop H and Scott E K 2017 Optical trapping of otoliths drives vestibular behaviours in larval zebrafish *Nat. Commun.* **8** 630
[47] Ashkin A and Dziedzic J M 1989 Optical trapping and manipulation of single living cells using infra-red laser beams *Ber. Bunsenges. Phys. Chem.* **93** 254–60
[48] Liu Y, Cheng D K, Sonek G J, Berns M W, Chapman C F and Tromberg B J 1995 Evidence for localized cell heating induced by infrared optical tweezers *Biophys. J.* **68** 2137–44
[49] Liang H, Vu K T, Krishnan P, Trang T C, Shin D, Kimel S and Berns M W 1996 Wavelength dependence of cell cloning efficiency after optical trapping *Biophys. J.* **70** 1529–33
[50] Leitz G, Fällman E, Tuck S and Axner O 2002 Stress response in *Caenorhabditis elegans* caused by optical tweezers: wavelength, power, and time dependence *Biophys. J.* **82** 2224–31
[51] Ayano S, Wakamoto Y, Yamashita S and Yasuda K 2006 Quantitative measurement of damage caused by 1064-nm wavelength optical trapping of *Escherichia coli* cells using on-chip single cell cultivation system *Biochem. Biophys. Res. Commun.* **350** 678–84
[52] Chiou P Y, Ohta A T and Wu M C 2005 Massively parallel manipulation of single cells and microparticles using optical images *Nature* **436** 370–2
[53] Lau A N K, Ohta A T, Phan H L, Hsu H Y, Jamshidi A, Chiou P Y and Wu M C 2009 Antifouling coatings for optoelectronic tweezers *Lab Chip* **9** 2952–7
[54] Probst C, Grünberger A, Wiechert W and Kohlheyer D 2013 Microfluidic growth chambers with optical tweezers for full spatial single-cell control and analysis of evolving microbes *J. Microbiol. Methods* **95** 470–6
[55] Wiklund M 2012 Acoustofluidics 12: biocompatibility and cell viability in microfluidic acoustic resonators *Lab Chip* **12** 2018–28
[56] Sundvik M, Nieminen H J, Salmi A, Panula P and Hæggström E 2015 Effects of acoustic levitation on the development of zebrafish, *Danio rerio*, embryos *Sci. Rep.* **5** 13596
[57] Lam K H, Li Y, Li Y, Lim H G, Zhou Q F and Shung K K 2016 Multifunctional single beam acoustic tweezer for non-invasive cell/organism manipulation and tissue imaging *Sci. Rep.* **6** 37554
[58] Ozcelik A, Rufo J, Guo F, Gu Y Y, Li P, Lata J and Huang T J 2018 Acoustic tweezers for the life sciences *Nat. Methods* **15** 1021–8
[59] Ding X Y, Lin S C S, Kiraly B, Yue H J, Li S X, Chiang I K, Shi J J, Benkovic S J and Huang T J 2012 On-chip manipulation of single microparticles, cells, and organisms using surface acoustic waves *Proc. Natl Acad. Sci. USA* **109** 11105–9
[60] Collins D J, Morahan B, Garcia-Bustos J, Doerig C, Plebanski M and Neild A 2015 Two-dimensional single-cell patterning with one cell per well driven by surface acoustic waves *Nat. Commun.* **6** 8686
[61] Guo F *et al* 2016 Three-dimensional manipulation of single cells using surface acoustic waves *Proc. Natl Acad. Sci. USA* **113** 1522–7
[62] Baudoin M, Thomas J L, Sahely R A, Gerbedoen J C, Gong Z X, Sivery A, Matar O B, Smagin N, Favreau P and Vlandas A 2020 Spatially selective manipulation of cells with single-beam acoustical tweezers *Nat. Commun.* **11** 4244
[63] Gartner Z J and Bertozzi C R 2009 Programmed assembly of 3-dimensional microtissues with defined cellular connectivity *Proc. Natl Acad. Sci. USA* **106** 4606–10
[64] Ge Z L, Liu J B, Guo L J, Yao G B, Li Q, Wang L H, Li J and Fan C H 2020 Programming cell–cell communications with engineered cell origami clusters *J. Am. Chem. Soc.* **142** 8800–8
[65] Wang B, Song J Z, Yuan H X, Nie C Y, Lv F T, Liu L B and Wang S 2014 Multicellular assembly and light-regulation of cell–cell communication by conjugated polymer materials *Adv. Mater.* **26** 2371–5
[66] O'Brien P J, Luo W, Rogozhnikov D, Chen J and Yousaf M N 2015 Spheroid and tissue assembly via click chemistry in microfluidic flow *Bioconjug. Chem.* **26** 1939–49
[67] Kim C H, Axup J Y, Dubrovska A, Kazane S A, Hutchins B A, Wold E D, Smider V V and Schultz P G 2012 Synthesis of bispecific antibodies using genetically encoded unnatural amino acids *J. Am. Chem. Soc.* **134** 9918–21
[68] Yüz S G, Rasoulinejad S, Mueller M, Wegner A E and Wegner S V 2019 Blue light switchable cell–cell interactions provide reversible and spatiotemporal control towards bottom-up tissue engineering *Adv. Biosyst.* **3** 1800310
[69] Hohnadel M, Maumy M, Chollet R and Chalmers J 2018 Development of a micromanipulation method for single cell isolation of prokaryotes and its application in food safety *PLoS One* **13** e0198208
[70] Hacohen A, Jessel H R, Richter-Levin A and Shefi O 2020 Patterning of particles and live cells at single cell resolution *Micromachines* **11** 505
[71] McCormack A, Highley C B, Leslie N R and Melchels F P W 2020 3D printing in suspension baths: keeping the promises of bioprinting afloat *Trends Biotechnol.* **38** 584–93
[72] Ellison S T, Duraivel S, Subramaniam V, Hugosson F, Yu B, Lebowitz J J, Khoshbouei H, Lele T P, Martindale M Q and Angelini T E 2022 Cellular micromasonry: biofabrication with single cell precision *Soft Matter* **18** 8554–60
[73] Ayan B, Heo D N, Zhang Z F, Dey M, Povilianskas A, Drapaca C and Ozbolat I T 2020 Aspiration-assisted bioprinting for precise positioning of biologics *Sci. Adv.* **6** eaaw5111
[74] Nakamura M, Kobayashi A, Takagi F, Watanabe A, Hiruma Y, Ohuchi K, Iwasaki Y, Horie M, Morita I and Takatani S 2005 Biocompatible inkjet printing technique for designed seeding of individual living cells *Tissue Eng.* **11** 1658–66
[75] Barron J A, Wu P, Ladouceur H D and Ringeisen B R 2004 Biological laser printing: a novel technique for creating heterogeneous 3-dimensional cell patterns *Biomed. Microdevices* **6** 139–47

[76] Xu T, Petridou S, Lee E H, Roth E A, Vyavahare N R, Hickman J J and Boland T 2004 Construction of high-density bacterial colony arrays and patterns by the ink-jet method *Biotechnol. Bioeng.* **85** 29–33

[77] Demirci U and Montesano G 2007 Single cell epitaxy by acoustic picolitre droplets *Lab Chip* **7** 1139–45

[78] Xu T, Kincaid H, Atala A and Yoo J J 2008 High-throughput production of single-cell microparticles using an inkjet printing technology *J. Manuf. Sci. Eng.* **130** 021017

[79] Guillotin B *et al* 2010 Laser assisted bioprinting of engineered tissue with high cell density and microscale organization *Biomaterials* **31** 7250–6

[80] Barron J A, Krizman D B and Ringeisen B R 2005 Laser printing of single cells: statistical analysis, cell viability, and stress *Ann. Biomed. Eng.* **33** 121–30

[81] Demirci U and Montesano G 2007 Cell encapsulating droplet vitrification *Lab Chip* **7** 1428–33

[82] Liu T-K, Pang Y, Zhou Z-Z, Yao R and Sun W 2019 An integrated cell printing system for the construction of heterogeneous tissue models *Acta Biomater.* **95** 245–57

[83] Mi S L, Yang S T, Liu T K, Du Z C, Xu Y Y, Li B H and Sun W 2019 A novel controllable cell array printing technique on microfluidic chips *IEEE Trans. Biomed. Eng.* **66** 2512–20

[84] Zhou D Z, Chen J W, Liu B X, Zhang X Z, Li X D and Xu T 2019 Bioinks for jet-based bioprinting *Bioprinting* **16** e00060

[85] Hospodiuk M, Dey M, Sosnoski D and Ozbolat I T 2017 The bioink: a comprehensive review on bioprintable materials *Biotechnol. Adv.* **35** 217–39

[86] Jentsch S, Nasehi R, Kuckelkorn C, Gundert B, Aveic S and Fischer H 2021 Multiscale 3D bioprinting by nozzle-free acoustic droplet ejection *Small Methods* **5** 2000971

[87] Zhang J, Byers P, Erben A, Frank C, Schulte-spechtel L, Heymann M, Docheva D, Huber H P, Sudhop S and Clausen-schaumann H 2021 Single cell bioprinting with ultrashort laser pulses *Adv. Funct. Mater.* **31** 2100066

[88] Ceyhan E, Xu F, Gurkan U A, Emre A E, Turali E S, El Assal R, Acikgenc A, Wu C-A M and Demirci U 2012 Prediction and control of number of cells in microdroplets by stochastic modeling *Lab Chip* **12** 4884–93

[89] Feng L, Sun Y L, Ohsumi C and Arai F 2013 Accurate dispensing system for single oocytes using air ejection *Biomicrofluidics* **7** 054113

[90] Schoendube J, Wright D, Zengerle R and Koltay P 2015 Single-cell printing based on impedance detection *Biomicrofluidics* **9** 014117

[91] Yusof A, Keegan H, Spillane C D, Sheils O M, Martin C M, O'Leary J J, Zengerle R and Koltay P 2011 Inkjet-like printing of single-cells *Lab Chip* **11** 2447–54

[92] Leibacher I, Schoendube J, Dual J, Zengerle R and Koltay P 2015 Enhanced single-cell printing by acoustophoretic cell focusing *Biomicrofluidics* **9** 024109

[93] Wang Y M, Wang X J, Pan T R, Li B Q and Chu J R 2021 Label-free single-cell isolation enabled by microfluidic impact printing and real-time cellular recognition *Lab Chip* **21** 3695–706

[94] Deng Y, Renaud P, Guo Z N, Huang Z G and Chen Y 2017 Single cell isolation process with laser induced forward transfer *J. Biol. Eng.* **11** 2

[95] Zhou Y C, He M H and Duan X X 2021 100% single cell encapsulation via acoustofluidic printing based on a gigahertz acoustic resonator *2021 43rd Annual Int. Conf. IEEE Engineering in Medicine & Biology Society (EMBC)* (IEEE) pp 1172–5

[96] Gross A, Schöndube J, Niekrawitz S, Streule W, Riegger L, Zengerle R and Koltay P 2013 Single-cell printer: automated, on demand, and label free *SLAS Technol.* **18** 504–18

[97] Nan L, Lai M Y A, Tang M Y H, Chan Y K, Poon L L M and Shum H C 2020 On-demand droplet collection for capturing single cells *Small* **16** 1902889

[98] Riba J, Schoendube J, Zimmermann S, Koltay P and Zengerle R 2020 Single-cell dispensing and 'real-time' cell classification using convolutional neural networks for higher efficiency in single-cell cloning *Sci. Rep.* **10** 1193

[99] Riba J, Gleichmann T, Zimmermann S, Zengerle R and Koltay P 2016 Label-free isolation and deposition of single bacterial cells from heterogeneous samples for clonal culturing *Sci. Rep.* **6** 32837

[100] Zhang P F and Abate A R 2020 High-definition single-cell printing: cell-by-cell fabrication of biological structures *Adv. Mater.* **32** 2005346

[101] Cole R H, Tang S Y, Siltanen C A, Shahi P, Zhang J Q, Poust S, Gartner Z J and Abate A R 2017 Printed droplet microfluidics for on demand dispensing of picoliter droplets and cells *Proc. Natl Acad. Sci. USA* **114** 8728–33

[102] He M Y, Edgar J S, Jeffries G D M, Lorenz R M, Shelby J P and Chiu D T 2005 Selective encapsulation of single cells and subcellular organelles into picoliter- and femtoliter-volume droplets *Anal. Chem.* **77** 1539–44

[103] Tan Y C, Hettiarachchi K, Siu M, Pan Y R and Lee A P 2006 Controlled microfluidic encapsulation of cells, proteins, and microbeads in lipid vesicles *J. Am. Chem. Soc.* **128** 5656–8

[104] Collins D J, Neild A, deMello A, Liu A Q and Ai Y 2015 The Poisson distribution and beyond: methods for microfluidic droplet production and single cell encapsulation *Lab Chip* **15** 3439–59

[105] Kamperman T, Henke S, van den Berg A, Shin S R, Tamayol A, Khademhosseini A, Karperien M and Leijten J 2017 Single cell microgel based modular bioinks for uncoupled cellular micro- and macroenvironments *Adv. Healthcare Mater.* **6** 1600913

[106] Kemna E W M, Schoeman R M, Wolbers F, Vermes I, Weitz D A and van den Berg A 2012 High-yield cell ordering and deterministic cell-in-droplet encapsulation using dean flow in a curved microchannel *Lab Chip* **12** 2881–7

[107] Mao A S *et al* 2017 Deterministic encapsulation of single cells in thin tunable microgels for niche modelling and therapeutic delivery *Nat. Mater.* **16** 236–43

[108] Lienemann P S, Rossow T, Mao A S, Vallmajo-Martin Q, Ehrbar M and Mooney D J 2017 Single cell-laden protease-sensitive microniches for long-term culture in 3D *Lab Chip* **17** 727–37

[109] Huang H S, Yu Y, Hu Y, He X M, Berk Usta O and Yarmush M L 2017 Generation and manipulation of hydrogel microcapsules by droplet-based microfluidics for mammalian cell culture *Lab Chip* **17** 1913–32

[110] Rommel D, Mork M, Vedaraman S, Bastard C, Guerzoni L P B, Kittel Y, Vinokur R, Born N, Haraszti T and De Laporte L 2022 Functionalized microgel rods interlinked into soft macroporous structures for 3D cell culture *Adv. Sci.* **9** 2103554

[111] Ma S H, Natoli M, Liu X, Neubauer M P, Watt F M, Fery A and Huck W T S 2013 Monodisperse collagen–gelatin beads as potential platforms for 3D cell culturing *J. Mater. Chem.* B **1** 5128–36

[112] Zhang L Y *et al* 2018 Microfluidic templated multicompartment microgels for 3D encapsulation and pairing of single cells *Small* **14** 1702955

[113] Kamperman T, Henke S, Visser C W, Karperien M and Leijten J 2017 Centering single cells in microgels via delayed crosslinking supports long-term 3D culture by preventing cell escape *Small* **13** 1603711

[114] Li Y, Shen Q, Shen J, Ding X B, Liu T, He J H, Zhu C Y, Zhao D and Zhu J D 2021 Multifunctional fibroblasts enhanced via thermal and freeze-drying post-treatments of aligned electrospun nanofiber membranes *Adv. Fiber Mater.* **3** 26–37
[115] Seymour A J, Westerfield A D, Cornelius V C, Skylar-Scott M A and Heilshorn S C 2022 Bioprinted microvasculature: progressing from structure to function *Biofabrication* **14** 022002
[116] Neal D, Sakar M S, Ong L-L S and Harry Asada H 2014 Formation of elongated fascicle-inspired 3D tissues consisting of high-density, aligned cells using sacrificial outer molding *Lab Chip* **14** 1907–16
[117] Saeki K, Hiramatsu H, Hori A, Hirai Y, Yamada M, Utoh R and Seki M 2020 Sacrificial alginate-assisted microfluidic engineering of cell-supportive protein microfibers for hydrogel-based cell encapsulation *ACS Omega* **5** 21641–50
[118] Ouyang L L 2022 Pushing the rheological and mechanical boundaries of extrusion-based 3D bioprinting *Trends Biotechnol.* **40** 891–902
[119] Zhang Y S, Haghiashtiani G, Hübscher T, Kelly D J, Lee J M, Lutolf M, McAlpine M C, Yeong W Y, Zenobi-Wong M and Malda J 2021 3D extrusion bioprinting *Nat. Rev. Methods Primers* **1** 75
[120] Shyam Mohan T, Datta P, Nesaei S, Ozbolat V and Ozbolat I T 2022 3D coaxial bioprinting: process mechanisms, bioinks and applications *Prog. Biomed. Eng.* **4** 022003
[121] Kang D G, Ahn G, Kim D, Kang H-W, Yun S, Yun W-S, Shim J-H and Jin S W 2018 Pre-set extrusion bioprinting for multiscale heterogeneous tissue structure fabrication *Biofabrication* **10** 035008
[122] Chang R, Nam J and Sun W 2008 Effects of dispensing pressure and nozzle diameter on cell survival from solid freeform fabrication–based direct cell writing *Tissue Eng.* A **14** 41–48
[123] Smith C M, Stone A L, Parkhill R L, Stewart R L, Simpkins M W, Kachurin A M, Warren W L and Williams S K 2004 Three-dimensional bioassembly tool for generating viable tissue-engineered constructs *Tissue Eng.* **10** 1566–76
[124] Ouyang L L, Highley C B, Sun W and Burdick J A 2017 A generalizable strategy for the 3D bioprinting of hydrogels from nonviscous photo-crosslinkable inks *Adv. Mater.* **29** 1604983
[125] Jeon O, Lee Y B, Jeong H, Lee S J, Wells D and Alsberg E 2019 Individual cell-only bioink and photocurable supporting medium for 3D printing and generation of engineered tissues with complex geometries *Mater. Horiz.* **6** 1625–31
[126] Lee A, Hudson A R, Shiwarski D J, Tashman J W, Hinton T J, Yerneni S, Bliley J M, Campbell P G and Feinberg A W 2019 3D bioprinting of collagen to rebuild components of the human heart *Science* **365** 482–7
[127] Reid J A, Mollica P A, Johnson G D, Ogle R C, Bruno R D and Sachs P C 2016 Accessible bioprinting: adaptation of a low-cost 3D-printer for precise cell placement and stem cell differentiation *Biofabrication* **8** 025017
[128] Huang J J, Wu J, Wang J H, Xu M J, Jiao J, Qiang Y H, Zhang F and Li Z 2023 Rock climbing-inspired electrohydrodynamic cryoprinting of micropatterned porous fiber scaffolds with improved MSC therapy for wound healing *Adv. Fiber Mater.* **5** 312–26
[129] Zong D D, Zhang X X, Yin X, Wang F, Yu J Y, Zhang S C and Ding B 2022 Electrospun fibrous sponges: principle, fabrication, and applications *Adv. Fiber Mater.* **4** 1434–62
[130] Onses M S, Sutanto E, Ferreira P M, Alleyne A G and Rogers J A 2015 Mechanisms, capabilities, and applications of high-resolution electrohydrodynamic jet printing *Small* **11** 4237–66
[131] Zhang B, He J K, Li X, Xu F Y and Li D C 2016 Micro/nanoscale electrohydrodynamic printing: from 2D to 3D *Nanoscale* **8** 15376–88
[132] Ehler E and Jayasinghe S N 2014 Cell electrospinning cardiac patches for tissue engineering the heart *Analyst* **139** 4449–52
[133] He J K, Zhao X, Chang J K and Li D C 2017 Microscale electro-hydrodynamic cell printing with high viability *Small* **13** 1702626
[134] Yeo M, Ha J, Lee H and Kim G 2016 Fabrication of hASCs-laden structures using extrusion-based cell printing supplemented with an electric field *Acta Biomater.* **38** 33–43
[135] Jayasinghe S N, Qureshi A N and Eagles P A M 2006 Electrohydrodynamic jet processing: an advanced electric-field-driven jetting phenomenon for processing living cells *Small* **2** 216–9
[136] Townsend-Nicholson A and Jayasinghe S N 2006 Cell electrospinning: a unique biotechnique for encapsulating living organisms for generating active biological microthreads/scaffolds *Biomacromolecules* **7** 3364–9
[137] Chen H P, Liu Y Y and Hu Q X 2015 A novel bioactive membrane by cell electrospinning *Exp. Cell Res.* **338** 261–6
[138] Jayasinghe S N, Auguste J and Scotton C J 2015 Platform technologies for directly reconstructing 3D living biomaterials *Adv. Mater.* **27** 7794–9
[139] Jayasinghe S N 2013 Cell electrospinning: a novel tool for functionalising fibres, scaffolds and membranes with living cells and other advanced materials for regenerative biology and medicine *Analyst* **138** 2215–23
[140] Yeo M and Kim G H 2018 Anisotropically aligned cell-laden nanofibrous bundle fabricated via cell electrospinning to regenerate skeletal muscle tissue *Small* **14** 1803491
[141] Qiu Z N, Zhu H, Wang Y T, Kasimu A, Li D C and He J K 2023 Functionalized alginate-based bioinks for microscale electrohydrodynamic bioprinting of living tissue constructs with improved cellular spreading and alignment *Bio-Des. Manuf.* **6** 136–49
[142] Wang M, Jin H J, Kaplan D L and Rutledge G C 2004 Mechanical properties of electrospun silk fibers *Macromolecules* **37** 6856–64
[143] Saquing C D, Tang C, Monian B, Bonino C A, Manasco J L, Alsberg E and Khan S A 2013 Alginate–polyethylene oxide blend nanofibers and the role of the carrier polymer in electrospinning *Ind. Eng. Chem. Res.* **52** 8692–704
[144] Castilho M, Levato R, Bernal P N, de Ruijter M, Sheng C Y, van Duijn J, Piluso S, Ito K and Malda J 2021 Hydrogel-based bioinks for cell electrowriting of well-organized living structures with micrometer-scale resolution *Biomacromolecules* **22** 855–66
[145] Yeo M and Kim G 2015 Fabrication of cell-laden electrospun hybrid scaffolds of alginate-based bioink and PCL microstructures for tissue regeneration *Chem. Eng. J.* **275** 27–35
[146] Gao Q, Xie C Q, Wang P, Xie M J, Li H B, Sun A Y, Fu J Z and He Y 2020 3D printed multi-scale scaffolds with ultrafine fibers for providing excellent biocompatibility *Mater. Sci. Eng.* C **107** 110269
[147] Yeo M and Kim G 2020 Micro/nano-hierarchical scaffold fabricated using a cell electrospinning/3D printing process for co-culturing myoblasts and HUVECs to induce myoblast alignment and differentiation *Acta Biomater.* **107** 102–14
[148] Wang C J, Xu Y Y, Xia J J, Zhou Z Z, Fang Y C, Zhang L and Sun W 2021 Multi-scale hierarchical scaffolds with

aligned micro-fibers for promoting cell alignment *Biomed. Mater.* **16** 045047
[149] Huang Y A *et al* 2021 Programmable robotized 'transfer-and-jet' printing for large, 3D curved electronics on complex surfaces *Int. J. Extrem. Manuf.* **3** 045101
[150] Shen C, Zhang G L, Wang Q C and Meng Q 2015 Fabrication of collagen gel hollow fibers by covalent cross-linking for construction of bioengineering renal tubules *ACS Appl. Mater. Interfaces* **7** 19789–97
[151] Lee B R, Lee K H, Kang E, Kim D S and Lee S H 2011 Microfluidic wet spinning of chitosan-alginate microfibers and encapsulation of HepG2 cells in fibers *Biomicrofluidics* **5** 022208
[152] Zuo Y C, He X H, Yang Y, Wei D, Sun J, Zhong M L, Xie R, Fan H S and Zhang X D 2016 Microfluidic-based generation of functional microfibers for biomimetic complex tissue construction *Acta Biomater.* **38** 153–62
[153] Lu B C, Li M F, Fang Y C, Liu Z B, Zhang T and Xiong Z 2021 Rapid fabrication of cell-laden microfibers for construction of aligned biomimetic tissue *Front. Bioeng. Biotechnol.* **8** 610249
[154] Wang G, Jia L L, Han F X, Wang J Y, Yu L, Yu Y K, Turnbull G, Guo M Y, Shu W M and Li B 2019 Microfluidics-based fabrication of cell-laden hydrogel microfibers for potential applications in tissue engineering *Molecules* **24** 1633
[155] Yamada M, Sugaya S, Naganuma Y and Seki M 2012 Microfluidic synthesis of chemically and physically anisotropic hydrogel microfibers for guided cell growth and networking *Soft Matter* **8** 3122–30
[156] Xie R X *et al* 2021 Composable microfluidic spinning platforms for facile production of biomimetic perfusable hydrogel microtubes *Nat. Protocols* **16** 937–64
[157] Yao K, Li W, Li K Y, Wu Q R, Gu Y R, Zhao L J, Zhang Y and Gao X H 2020 Simple fabrication of multicomponent heterogeneous fibers for cell co-culture via microfluidic spinning *Macromol. Biosci.* **20** 1900395
[158] Takahashi K, Takao H, Shimokawa F and Terao K 2022 On-demand formation of heterogeneous gel fibers using two-dimensional micronozzle array *Microfluid. Nanofluid.* **26** 15
[159] Lee J M, Sing S L, Zhou M M and Yeong W Y 2018 3D bioprinting processes: a perspective on classification and terminology *Int. J. Bioprint.* **4** 151
[160] Kim S H *et al* 2018 Precisely printable and biocompatible silk fibroin bioink for digital light processing 3D printing *Nat. Commun.* **9** 1620
[161] Zhu W *et al* 2017 Direct 3D bioprinting of prevascularized tissue constructs with complex microarchitecture *Biomaterials* **124** 106–15
[162] Okano T, Yamada N, Sakai H and Sakurai Y 1993 A novel recovery system for cultured cells using plasma-treated polystyrene dishes grafted with poly(N-isopropylacrylamide) *J. Biomed. Mater. Res.* **27** 1243–51
[163] Yamada N, Okano T, Sakai H, Karikusa F, Sawasaki Y and Sakurai Y 1990 Thermo-responsive polymeric surfaces; control of attachment and detachment of cultured cells *Makromol. Chem. Rapid Commun.* **11** 571–6
[164] Mizutani A, Kikuchi A, Yamato M, Kanazawa H and Okano T 2008 Preparation of thermoresponsive polymer brush surfaces and their interaction with cells *Biomaterials* **29** 2073–81
[165] Arisaka Y, Kobayashi J, Yamato M, Akiyama Y and Okano T 2013 Switching of cell growth/detachment on heparin-functionalized thermoresponsive surface for rapid cell sheet fabrication and manipulation *Biomaterials* **34** 4214–22
[166] Dzhoyashvili N A, Thompson K, Gorelov A V and Rochev Y A 2016 Film thickness determines cell growth and cell sheet detachment from spin-coated poly(*N*-isopropylacrylamide) substrates *ACS Appl. Mater. Interfaces* **8** 27564–72
[167] Kikuchi A and Okano T 2005 Nanostructured designs of biomedical materials: applications of cell sheet engineering to functional regenerative tissues and organs *J. Control. Release* **101** 69–84
[168] Akiyama Y, Matsuyama M, Yamato M, Takeda N and Okano T 2018 Poly(*N*-isopropylacrylamide)-grafted polydimethylsiloxane substrate for controlling cell adhesion and detachment by dual stimulation of temperature and mechanical stress *Biomacromolecules* **19** 4014–22
[169] Bonetti L, De Nardo L and Farè S 2021 Chemically crosslinked methylcellulose substrates for cell sheet engineering *Gels* **7** 141
[170] Altomare L, Cochis A, Carletta A, Rimondini L and Farè S 2016 Thermo-responsive methylcellulose hydrogels as temporary substrate for cell sheet biofabrication *J. Mater. Sci. Mater. Med.* **27** 95
[171] Hong Y, Yu M F, Weng W J, Cheng K, Wang H M and Lin J 2013 Light-induced cell detachment for cell sheet technology *Biomaterials* **34** 11–18
[172] Wang X Z, Cheng K, Weng W J, Wang H M and Lin J 2016 Light-induced cell-sheet harvest on TiO_2 films sensitized with carbon quantum dots *ChemPlusChem* **81** 1166–73
[173] Wang X Z, Yao C, Weng W J, Cheng K and Wang Q 2017 Visible-light-responsive surfaces for efficient, noninvasive cell sheet harvesting *ACS Appl. Mater. Interfaces* **9** 28250–9
[174] Kim J D, Heo J S, Park T, Park C, Kim H O and Kim E 2015 Photothermally induced local dissociation of collagens for harvesting of cell sheets *Angew. Chem., Int. Ed.* **54** 5869–73
[175] Koo M A, Lee M H, Kwon B J, Seon G M, Kim M S, Kim D, Nam K C and Park J C 2018 Exogenous ROS-induced cell sheet transfer based on hematoporphyrin-polyketone film via a one-step process *Biomaterials* **161** 47–56
[176] Koo M A, Hee Hong S, Hee Lee M, Kwon B J, Mi Seon G, Sung Kim M, Kim D, Chang Nam K and Park J C 2019 Effective stacking and transplantation of stem cell sheets using exogenous ROS-producing film for accelerated wound healing *Acta Biomater.* **95** 418–26
[177] Koo M A, Lee M H and Park J C 2019 Recent advances in ROS-responsive cell sheet techniques for tissue engineering *Int. J. Mol. Sci.* **20** 5656
[178] Zhang W J, Yang G Z, Wang X S, Jiang L T, Jiang F, Li G L, Zhang Z Y and Jiang X Q 2017 Magnetically controlled growth-factor-immobilized multilayer cell sheets for complex tissue regeneration *Adv. Mater.* **29** 1703795
[179] Ito A and Kamihira M 2011 Tissue engineering using magnetite nanoparticles *Progress in Molecular Biology and Translational Science* vol 104 (Academic Press Inc Elsevier Science) pp 355–95
[180] Yamamoto Y, Ito A, Kato M, Kawabe Y, Shimizu K, Fujita H, Nagamori E and Kamihira M 2009 Preparation of artificial skeletal muscle tissues by a magnetic force-based tissue engineering technique *J. Biosci. Bioeng.* **108** 538–43
[181] Gonçalves A I, Rodrigues M T and Gomes M E 2017 Tissue-engineered magnetic cell sheet patches for advanced strategies in tendon regeneration *Acta Biomater.* **63** 110–22
[182] Koto W, Shinohara Y, Kitamura K, Wachi T, Makihira S and Koyano K 2017 Porcine dental epithelial cells differentiated in a cell sheet constructed by magnetic nanotechnology *Nanomaterials* **7** 322
[183] Silva A S, Santos L F, Mendes M C and Mano J F 2020 Multi-layer pre-vascularized magnetic cell sheets for bone regeneration *Biomaterials* **231** 119664

[184] Cochran D B, Wattamwar P P, Wydra R, Hilt J Z, Anderson K W, Eitel R E and Dziubla T D 2013 Suppressing iron oxide nanoparticle toxicity by vascular targeted antioxidant polymer nanoparticles *Biomaterials* **34** 9615–3622
[185] Iwata T, Yamato M, Tsuchioka H, Takagi R, Mukobata S, Washio K, Okano T and Ishikawa I 2009 Periodontal regeneration with multi-layered periodontal ligament-derived cell sheets in a canine model *Biomaterials* **30** 2716–23
[186] Gauvin R, Ahsan T, Larouche D, Lévesque P, Dubé J, Auger F A, Nerem R M and Germain L 2010 A novel single-step self-assembly approach for the fabrication of tissue-engineered vascular constructs *Tissue Eng.* A **16** 1737–47
[187] Yu J, Wang M Y, Tai H C and Cheng N C 2018 Cell sheet composed of adipose-derived stem cells demonstrates enhanced skin wound healing with reduced scar formation *Acta Biomater.* **77** 191–200
[188] Kang Y Q, Ren L L and Yang Y Z 2014 Engineering vascularized bone grafts by integrating a biomimetic periosteum and β-TCP scaffold *ACS Appl. Mater. Interfaces* **6** 9622–33
[189] Kobayashi J, Kikuchi A, Aoyagi T and Okano T 2019 Cell sheet tissue engineering: cell sheet preparation, harvesting/manipulation, and transplantation *J. Biomed. Mater. Res.* A **107** 955–67
[190] Ronfard V, Broly H, Mitchell V, Galizia J P, Hochart D, Chambon E, Pellerin P and Huart J J 1991 Use of human keratinocytes cultured on fibrin glue in the treatment of burn wounds *Burns* **17** 181–4
[191] Inaba R, Khademhosseini A, Suzuki H and Fukuda J 2009 Electrochemical desorption of self-assembled monolayers for engineering cellular tissues *Biomaterials* **30** 3573–9
[192] Enomoto J, Kageyama T, Myasnikova D, Onishi K, Kobayashi Y, Taruno Y, Kanai T and Fukuda J 2018 Gold cleaning methods for preparation of cell culture surfaces for self-assembled monolayers of zwitterionic oligopeptides *J. Biosci. Bioeng.* **125** 606–12
[193] Zhang L B, Wang Z J, Das J, Labib M, Ahmed S, Sargent E H and Kelley S O 2019 Potential-responsive surfaces for manipulation of cell adhesion, release, and differentiation *Angew. Chem., Int. Ed.* **58** 14519–23
[194] Kurashina Y, Imashiro C, Hirano M, Kuribara T, Totani K, Ohnuma K, Friend J and Takemura K 2019 Enzyme-free release of adhered cells from standard culture dishes using intermittent ultrasonic traveling waves *Commun. Biol.* **2** 393
[195] Imashiro C, Hirano M, Morikura T, Fukuma Y, Ohnuma K, Kurashina Y, Miyata S and Takemura K 2020 Detachment of cell sheets from clinically ubiquitous cell culture vessels by ultrasonic vibration *Sci. Rep.* **10** 9468
[196] Ohashi K *et al* 2007 Engineering functional two- and three-dimensional liver systems *in vivo* using hepatic tissue sheets *Nat. Med.* **13** 880–5
[197] Kim M S, Lee B, Kim H N, Bang S, Yang H S, Kang S M, Suh K Y, Park S H and Jeon N L 2017 3D tissue formation by stacking detachable cell sheets formed on nanofiber mesh *Biofabrication* **9** 015029
[198] Haraguchi Y *et al* 2012 Fabrication of functional three-dimensional tissues by stacking cell sheets *in vitro* *Nat. Protocols* **7** 850–8
[199] Haraguchi Y, Kagawa Y, Hasegawa A, Kubo H and Shimizu T 2018 Rapid fabrication of detachable three-dimensional tissues by layering of cell sheets with heating centrifuge *Biotechnol. Prog.* **34** 692–701
[200] Tsuda Y, Shimizu T, Yamato M, Kikuchi A, Sasagawa T, Sekiya S, Kobayashi J, Chen G P and Okano T 2007 Cellular control of tissue architectures using a three-dimensional tissue fabrication technique *Biomaterials* **28** 4939–46
[201] Hannachi I E, Itoga K, Kumashiro Y, Kobayashi J, Yamato M and Okano T 2009 Fabrication of transferable micropatterned-co-cultured cell sheets with microcontact printing *Biomaterials* **30** 5427–32
[202] Sasagawa T, Shimizu T, Sekiya S, Haraguchi Y, Yamato M, Sawa Y and Okano T 2010 Design of prevascularized three-dimensional cell-dense tissues using a cell sheet stacking manipulation technology *Biomaterials* **31** 1646–54
[203] Asakawa N, Shimizu T, Tsuda Y, Sekiya S, Sasagawa T, Yamato M, Fukai F and Okano T 2010 Pre-vascularization of *in vitro* three-dimensional tissues created by cell sheet engineering *Biomaterials* **31** 3903–9
[204] Shimizu K, Ito A, Lee J K, Yoshida T, Miwa K, Ishiguro H, Numaguchi Y, Murohara T, Kodama I and Honda H 2007 Construction of multi-layered cardiomyocyte sheets using magnetite nanoparticles and magnetic force *Biotechnol. Bioeng.* **96** 803–9
[205] Ito A, Jitsunobu H, Kawabe Y and Kamihira M 2007 Construction of heterotypic cell sheets by magnetic force-based 3D coculture of HepG2 and NIH3T3 cells *J. Biosci. Bioeng.* **104** 371–8
[206] Lu Y Z *et al* 2021 A rapidly magnetically assembled stem cell microtissue with "hamburger" architecture and enhanced vascularization capacity *Bioact. Mater.* **6** 3756–65
[207] Santos L F, Patrício S G, Silva A S and Mano J F 2022 Freestanding magnetic microtissues for tissue engineering applications *Adv. Healthcare Mater.* **11** 2101532
[208] L'Heureux N, Pâquet S, Labbé R, Germain L and Auger F A 1998 A completely biological tissue-engineered human blood vessel *FASEB J.* **12** 47–56
[209] Jiang Z W, Yu K, Feng Y T, Zhang L F and Yang G L 2020 An effective light activated TiO_2 nanodot platform for gene delivery within cell sheets to enhance osseointegration *Chem. Eng. J.* **402** 126170
[210] Othman R, E, Morris G, Shah D A, Hall S, Hall G, Wells K, Shakesheff K M and Dixon J E 2015 An automated fabrication strategy to create patterned tubular architectures at cell and tissue scales *Biofabrication* **7** 025003
[211] Tanaka Y, Sato K, Shimizu T, Yamato M, Okano T and Kitamori T 2007 A micro-spherical heart pump powered by cultured cardiomyocytes *Lab Chip* **7** 207–12
[212] Ramadhan W, Kagawa G, Moriyama K, Wakabayashi R, Minamihata K, Goto M and Kamiya N 2020 Construction of higher-order cellular microstructures by a self-wrapping co-culture strategy using a redox-responsive hydrogel *Sci. Rep.* **10** 6710
[213] Abate M F, Jia S S, Ahmed M G, Li X R, Lin L, Chen X Q, Zhu Z and Yang C Y 2019 Visual quantitative detection of circulating tumor cells with single-cell sensitivity using a portable microfluidic device *Small* **15** 1804890
[214] Peng R, Yao X and Ding J D 2011 Effect of cell anisotropy on differentiation of stem cells on micropatterned surfaces through the controlled single cell adhesion *Biomaterials* **32** 8048–57
[215] Wang Y T, Yang Y J, Yoshitomi T, Kawazoe N, Yang Y N and Chen G P 2021 Regulation of gene transfection by cell size, shape and elongation on micropatterned surfaces *J. Mater. Chem.* B **9** 4329–39
[216] Chen Y C, Allen S G, Ingram P N, Buckanovich R, Merajver S D and Yoon E 2015 Single-cell migration chip for chemotaxis-based microfluidic selection of heterogeneous cell populations *Sci. Rep.* **5** 9980
[217] Schmitz J, Täuber S, Westerwalbesloh C, von Lieres E, Noll T and Grünberger A 2021 Development and

application of a cultivation platform for mammalian suspension cell lines with single-cell resolution *Biotechnol. Bioeng.* **118** 992–1005
[218] Lin D G, Li P W, Feng J, Lin Z, Chen X, Yang N, Wang L H and Liu D Y 2020 Screening therapeutic agents specific to breast cancer stem cells using a microfluidic single-cell clone-forming inhibition assay *Small* **16** 1901001
[219] Han K, Sun M L, Zhang J W, Fu W Z, Hu R, Liu D and Liu W M 2021 Large-scale investigation of single cell activities and response dynamics in a microarray chip with a microfluidics-fabricated microporous membrane *Analyst* **146** 4303–13
[220] Hsu M N, Wei S C, Guo S, Phan D T, Zhang Y and Chen C H 2018 Smart hydrogel microfluidics for single-cell multiplexed secretomic analysis with high sensitivity *Small* **14** 1802918
[221] de Wagenaar B, Berendsen J T W, Bomer J G, Olthuis W, van den Berg A and Segerink L I 2015 Microfluidic single sperm entrapment and analysis *Lab Chip* **15** 1294–301
[222] Friedlander T W, Premasekharan G and Paris P L 2014 Looking back, to the future of circulating tumor cells *Pharmacol. Ther.* **142** 271–80
[223] Sadoun A, Biarnes-Pelicot M, Ghesquiere-Dierickx L, Wu A, Théodoly O, Limozin L, Hamon Y and Puech P H 2021 Controlling T cells spreading, mechanics and activation by micropatterning *Sci. Rep.* **11** 6783
[224] Xu Z Y, Orkwis J A, DeVine B M and Harris G M 2020 Extracellular matrix cues modulate Schwann cell morphology, proliferation, and protein expression *J. Tissue Eng. Regen. Med.* **14** 229–42
[225] Von Erlach T C *et al* 2018 Cell-geometry-dependent changes in plasma membrane order direct stem cell signalling and fate *Nat. Mater.* **17** 237–42
[226] Yao X, Liu R L, Liang X Y and Ding J D 2019 Critical areas of proliferation of single cells on micropatterned surfaces and corresponding cell type dependence *ACS Appl. Mater. Interfaces* **11** 15366–80
[227] Lim S B, Di Lee W, Vasudevan J, Lim W-T and Lim C T 2019 Liquid biopsy: one cell at a time *npj Precis. Oncol.* **3** 23
[228] Alvarez-Elizondo M B, Li C W, Marom A, Tung Y-T, Drillich G, Horesh Y, Lin S C, Wang G-J and Weihs D 2020 Micropatterned topographies reveal measurable differences between cancer and benign cells *Med. Eng. Phys.* **75** 5–12
[229] Deng Y L *et al* 2014 An integrated microfluidic chip system for single-cell secretion profiling of rare circulating tumor cells *Sci. Rep.* **4** 7499
[230] Armbrecht L, Rutschmann O, Szczerba B M, Nikoloff J, Aceto N and Dittrich P S 2020 Quantification of protein secretion from circulating tumor cells in microfluidic chambers *Adv. Sci.* **7** 1903237
[231] Lin X X, Fang F X, Wang C J, Kankala R K and Zhou S F 2021 Inkjet printing-assisted single-cell microarray on a hydrophobic surface chip for real-time monitoring of enzyme kinetics at single-cell level *Talanta* **225** 122019
[232] Faroni A, Mobasseri S A, Kingham P J and Reid A J 2015 Peripheral nerve regeneration: experimental strategies and future perspectives *Adv. Drug. Deliv. Rev.* **82–83** 160–7
[233] Solanki A, Shah S, Memoli K A, Park S Y, Hong S and Lee K B 2010 Controlling differentiation of neural stem cells using extracellular matrix protein patterns *Small* **6** 2509–13
[234] Patil P, Szymanski J M and Feinberg A W 2016 Defined micropatterning of ECM protein adhesive sites on alginate microfibers for engineering highly anisotropic muscle cell bundles *Adv. Mater. Technol.* **1** 16000031
[235] Rayner S G, Howard C C, Mandrycky C J, Stamenkovic S, Himmelfarb J, Shih A Y and Zheng Y 2021 Multiphoton-guided creation of complex organ-specific microvasculature *Adv. Healthcare Mater.* **10** e2100031
[236] Sumide T *et al* 2006 Functional human corneal endothelial cell sheets harvested from temperature-responsive culture surfaces *FASEB J.* **20** 392–4
[237] Song S Y, Kim H, Yoo J, Kwon S P, Park B W, Kim J-J, Ban K, Char K, Park H-J and Kim B-S 2020 Prevascularized, multiple-layered cell sheets of direct cardiac reprogrammed cells for cardiac repair *Biomater. Sci.* **8** 4508–20
[238] Yeo M, Yoon J W, Park G T, Shin S C, Song Y C, Cheon Y I, Lee B J, Kim G H and Kim J H 2023 Esophageal wound healing by aligned smooth muscle cell-laden nanofibrous patch *Mater. Today Bio* **19** 100564
[239] Nishida K *et al* 2004 Corneal reconstruction with tissue-engineered cell sheets composed of autologous oral mucosal epithelium *New Engl. J. Med.* **351** 1187–96
[240] Nishida K *et al* 2004 Functional bioengineered corneal epithelial sheet grafts from corneal stem cells expanded *ex vivo* on a temperature-responsive cell culture surface *Transplantation* **77** 379–85
[241] Umemoto T, Yamato M, Nishida K and Okano T 2013 Regenerative medicine of cornea by cell sheet engineering using temperature-responsive culture surfaces *Chin. Sci. Bull.* **58** 4349–56
[242] Ide T, Nishida K, Yamato M, Sumide T, Utsumi M, Nozaki T, Kikuchi A, Okano T and Tano Y 2006 Structural characterization of bioengineered human corneal endothelial cell sheets fabricated on temperature-responsive culture dishes *Biomaterials* **27** 607–14
[243] Jia Y, Li W, Duan H, Li Z, Zhou Q and Shi W 2018 Mini-sheet injection for cultured corneal endothelial transplantation *Tissue Eng. Part C : Methods* **24** 474–9
[244] Sekine H, Shimizu T, Dobashi I, Matsuura K, Hagiwara N, Takahashi M, Kobayashi E, Yamato M and Okano T 2011 Cardiac cell sheet transplantation improves damaged heart function via superior cell survival in comparison with dissociated cell injection *Tissue Eng.* A **17** 2973–80
[245] Matsuura K, Haraguchi Y, Shimizu T and Okano T 2013 Cell sheet transplantation for heart tissue repair *J. Control. Release* **169** 336–40
[246] Sawa Y, Miyagawa S, Sakaguchi T, Fujita T, Matsuyama A, Saito A, Shimizu T and Okano T 2012 Tissue engineered myoblast sheets improved cardiac function sufficiently to discontinue LVAS in a patient with DCM: report of a case *Surg. Today* **42** 181–4
[247] Tanaka Y *et al* 2016 Autologous preconditioned mesenchymal stem cell sheets improve left ventricular function in a rabbit old myocardial infarction model *Am. J. Transl. Res.* **8** 2222–33
[248] Kawamura M *et al* 2017 Enhanced therapeutic effects of human iPS cell derived-cardiomyocyte by combined cell-sheets with omental flap technique in porcine ischemic cardiomyopathy model *Sci. Rep.* **7** 8824
[249] Kawamura M *et al* 2012 Feasibility, safety, and therapeutic efficacy of human induced pluripotent stem cell-derived cardiomyocyte sheets in a porcine ischemic cardiomyopathy model *Circulation* **126** S29–S37
[250] Guo R, Morimatsu M, Feng T, Lan F, Chang D H, Wan F and Ling Y P 2020 Stem cell-derived cell sheet transplantation for heart tissue repair in myocardial infarction *Stem Cell Res. Ther.* **11** 19
[251] Shimizu T *et al* 2015 The regeneration and augmentation of bone with injectable osteogenic cell sheet in a rat critical fracture healing model *Injury* **46** 1457–64
[252] Zhou L B, Ding R Y, Li B W, Han H L, Wang H N, Wang G, Xu B X, Zhai S Q and Wu W 2015 Cartilage engineering

using chondrocyte cell sheets and its application in reconstruction of microtia *Int. J. Clin. Exp. Pathol.* **8** 73–80
[253] Zhang H L, Zhou Y L, Zhang W, Wang K R, Xu L H, Ma H R and Deng Y 2018 Construction of vascularized tissue-engineered bone with a double-cell sheet complex *Acta Biomater.* **77** 212–27
[254] Xu M, Li J D, Liu X N, Long S Q, Shen Y, Li Q, Ren L L and Ma D Y 2019 Fabrication of vascularized and scaffold-free bone tissue using endothelial and osteogenic cells differentiated from bone marrow derived mesenchymal stem cells *Tissue Cell* **61** 21–29
[255] Lee J, Shin D and Roh J L 2018 Use of a pre-vascularised oral mucosal cell sheet for promoting cutaneous burn wound healing *Theranostics* **8** 5703–12
[256] Guo H L, Peng X F, Bao X Q, Wang L, Jia Z M, Huang Y C, Zhou J M, Xie H and Chen F 2020 Bladder reconstruction using autologous smooth muscle cell sheets grafted on a pre-vascularized capsule *Theranostics* **10** 10378–93
[257] Jia Z M, Guo H L, Xie H, Zhou J M, Wang Y P, Bao X Q, Huang Y C and Chen F 2019 Construction of pedicled smooth muscle tissues by combining the capsule tissue and cell sheet engineering *Cell Transplant.* **28** 328–42
[258] Yu M M, Chen J S, Wang L, Huang Y C, Xie H, Bian Y and Chen F 2022 Engineering pedicled vascularized bladder tissue for functional bladder defect repair *Bioeng. Transl. Med.* e10440
[259] Hofer M and Lutolf M P 2021 Engineering organoids *Nat. Rev. Mater.* **6** 402–20
[260] Shahbazi M N, Siggia E D and Zernicka-Goetz M 2019 Self-organization of stem cells into embryos: a window on early mammalian development *Science* **364** 948–51
[261] Arora N, Alsous J I, Guggenheim J W, Mak M, Munera J, Wells J M, Kamm R D, Asada H H, Shvartsman S Y and Griffith L G 2017 A process engineering approach to increase organoid yield *Development* **144** 1128–36
[262] Lancaster M A, Corsini N S, Wolfinger S, Gustafson E H, Phillips A W, Burkard T R, Otani T, Livesey F J and Knoblich J A 2017 Guided self-organization and cortical plate formation in human brain organoids *Nat. Biotechnol.* **35** 659–66
[263] van den Brink S C, Baillie-Johnson P, Balayo T, Hadjantonakis A K, Nowotschin S, Turner D A and Arias A M 2014 Symmetry breaking, germ layer specification and axial organisation in aggregates of mouse embryonic stem cells *Development* **141** 4231–42
[264] Kim E *et al* 2020 Creation of bladder assembloids mimicking tissue regeneration and cancer *Nature* **588** 664–9
[265] Liu Y *et al* 2021 Bio-assembling macro-scale, lumenized airway tubes of defined shape via multi-organoid patterning and fusion *Adv. Sci.* **8** 2003332